Title: Ribosome demand links transcriptional bursts to protein expression noise

Authors: Sampriti Pal[1], Upasana Ray[1], Riddhiman Dhar[1]*

Affiliations:

[1]Department of Bioscience and Biotechnology, IIT Kharagpur, India

*Corresponding author. Email: riddhiman.dhar@iitkgp.ac.in

Stochastic variation in protein expression generates phenotypic heterogeneity in a cell population and has an important role in antibiotic persistence, mutation penetrance, tumor growth and therapy resistance. Studies investigating molecular origins of noise have predominantly focused on the transcription process. However, the noise generated in the transcription process is further modulated by translation. This influences the expression noise at the protein level which eventually determines the extent of phenotypic heterogeneity in a cell population. Studies across different organisms have revealed a positive association between translational efficiency and protein noise. However, the molecular basis of this association has remained unknown. In this work, through stochastic modeling of translation in single mRNA molecules and empirical measurements of protein noise, we show that ribosome demand associated with high translational efficiency in a gene drives the correlation between translational efficiency and protein noise. We also show that this correlation is present only in genes with bursty transcription. Thus, our work reveals the molecular basis of how coding sequence of genes, along with their promoters, can regulate noise. These findings have important implications for investigating protein noise and phenotypic heterogeneity across biological systems.

Running Title: Translational control of gene expression noise

Keywords:

Protein expression noise; Transcriptional bursts; Translational bursts; Translational efficiency; Ribosome demand

Introduction

Genetically identical cells often show variation in gene expression under identical environmental condition. Stochastic variation in gene expression, termed as expression noise, generates phenotypic heterogeneity which has important implications for many biological processes. Gene expression noise has been associated with persistence of microbial cells in antibiotics[1,2], incomplete mutation penetrance[3-5], cellular decision-making[6,7], cancer progression, and anti-cancer therapy resistance[8-10]. Transcription occurring in bursts[11-13], with a promoter transitioning between on- and off-states, is a major source of expression noise, and each promoter has its characteristic burst frequency and burst size[14-18]. Earlier studies have associated presence of TATA box motif[19,20], occurrence of TFIID and SAGA co-activator complexes with TATA binding protein [21], nucleosome occupancy, and histone modifications with expression noise[22-25]. In addition, transcription factors (TFs) and the gene regulatory network play important roles in determining noise [26-28].

The expression noise generated by transcription is modulated by the translation process[13,29]. Thus, a gene that exhibits high expression noise at the mRNA level may not show high noise at the protein level. Two early studies observed a positive association between translational efficiency and expression noise in bacteria and yeast[30,31], where an increase in mean protein expression, engineered by changes in synonymous codons, led to an increase in expression noise. This contrasted with the traditional inverse relationship between mean protein expression and noise observed in empirical measurements of noise in bacteria and yeast[14-16]. Salari *et al.*[32], through a computational analysis of expression noise in yeast, observed an increase in positive correlation between tRNA adaptation index (tAI), a proxy for translational efficiency[33,34], and expression

54 noise for genes with tAI values up to 0.55. The correlation, however, decreased thereafter[32]. In
55 addition, a recent study in *Arabidopsis* reported a positive correlation between translational
56 efficiency and expression noise[35], similar to what had been observed in microbes. Taken together,
57 these studies showed that the translation process impacted protein expression noise in similar
58 manner across biological systems.
59
60 What is the molecular basis of the positive correlation between translational efficiency and protein
61 expression noise? The answer to this question remains unclear, although some mechanisms have
62 been proposed. To achieve a specific protein expression level, a cell can produce many mRNA
63 molecules and translate them at a low rate, or can start with a small number of mRNA molecules
64 and translate them at a high rate[36]. It has been argued that the latter scenario requiring high
65 translation rate may lead to more noise, due to constraints on availability of mRNA, or due to
66 fluctuations in small mRNA numbers[36,37]. However, there has only been indirect evidence in
67 support of this hypothesis[36]. Further, recent studies have shown that the translation process is
68 bursty in nature and can switch between on- and off-states[38,39], just like the transcription process.
69 Whether translational bursting along with transcriptional bursting can explain the correlation
70 between translational efficiency and noise remains unknown.
71
72 In this work, we show that fluctuations in mRNA levels, originating from bursty transcription,
73 combined with high translational efficiency can lead to high protein noise. Through stochastic
74 modeling of translation in single mRNA molecules, we uncovered that the extent of demand for
75 the ribosomal machinery needed for translation at the level of individual genes determined how
76 transcriptional noise was translated into protein noise. In addition, we found that the positive
77 association between translational efficiency and protein noise was visible only for genes that

showed bursty transcription. Consequently, the ribosome demand model predicted that a reduction in translational efficiency or a departure from bursty transcription to a more uniform rate of transcription would abolish the association between translational efficiency and protein noise. We validated both these predictions through an experimental noise measurement system in yeast, thereby establishing ribosome demand as the molecular link between transcriptional bursts and protein noise. Taken together, our work reveals the molecular basis of how coding sequence of genes can regulate protein noise via modulating the translation rate. These findings have implications for investigating protein noise and phenotypic heterogeneity across biological systems.

Results

High protein noise in genes with low transcription and high translation stems from high mRNA noise

We first tested the existing hypothesis which posits that the genes with low transcription and high translation would exhibit more protein expression noise than the genes with high transcription and low translation (Fig. 1A). Although it has been reported that essential genes in the yeast *Saccharomyces cerevisiae* employ high transcription and low translation strategy for expression, presumably because of detrimental effects of high noise in these genes[36], there is no direct supportive evidence. To test this hypothesis, we compared protein expression noise of genes showing different levels of transcription and translation in the yeast *S. cerevisiae*. We obtained the mRNA expression data from the study of Nadal-Ribelles *et al.*[40], who quantified mRNA expression at the level of single cells in yeast (Fig. S1A). We used the data on protein synthesis rate per mRNA from Riba *et al.*[41] as a measure of translational efficiency (Fig. S1B). We obtained the protein expression noise data from Newman *et al.*[15], and used their measure of Distance-to-

102 Median (DM), that is corrected for the dependence of expression noise (coefficient of variation,
103 CV = standard deviation of protein expression level/mean protein expression) on mean protein
104 expression, as the measure of protein noise. We obtained protein noise values of 2763 genes from
105 this dataset (Fig. S1C).
106
107 Mean mRNA expression and translational efficiency individually showed poor correlation with
108 protein noise (Fig. S2). We therefore classified yeast genes based on the quartiles of mean mRNA
109 expression values, and then by the quartiles of translational efficiency resulting in a total of 16
110 classes (Fig. 1B). The group of genes with low mean mRNA expression and high translational
111 efficiency showed significantly higher protein expression noise (DM, median noise = 3.02)
112 compared to the genes with high mRNA expression and low translational efficiency (median
113 protein noise = -0.724; Mann-Whitney U-test, p=0.001; Fig. 1B), suggesting that low mRNA
114 expression and high translational efficiency was indeed associated with high protein noise.
115
116 To better understand how low mRNA expression and high translational efficiency could lead to
117 high protein noise, we employed a two-state model of gene expression[42]. Briefly, a gene can switch
118 between on- and off-states with rates K_{on} and K_{off}, respectively (Fig. 1C). In the on-state, the gene
119 is transcribed at a rate β_m, and the mRNA molecules produced are translated at a rate β_p. Using
120 stochastic simulations following Gillespie's algorithm[43], we modeled the changes in
121 concentrations of mRNA and protein molecules over time individually in 1000 cells, and further
122 calculated mean protein expression and noise values (coefficient of variation, CV) (see Methods).
123 In all simulations, we quantified protein expression noise by coefficient of variation as it was not
124 possible to calculate mean-adjusted noise or DM for a single gene. We modeled the impact of
125 mRNA expression and translational efficiency on expression noise by varying the transcription

126 (β_m) and the translation (β_p) rates over a wide range of values (Fig. 1D). However, we did not see
127 any change in protein noise, either with changes in the translation rate for a specific mean mRNA
128 expression, or with changes in the mean mRNA expression (CV= ~0.62, Fig. 1D). Further,
129 simulations over a wide-range of burst frequencies (K_{on}) did not reveal any correlation between
130 translational efficiency and protein noise (Fig. 1E). These results suggested that the differences in
131 the mRNA levels and the translational efficiency could not explain the differences in noise values
132 between low-mRNA high-translation class compared to the high-mRNA low-translation class.
133
134 Next, we tested whether higher heterogeneity in mRNA numbers associated with low mean mRNA
135 expression could explain the higher protein noise in the genes of the low-mRNA high-translation
136 class[37] from the experimental data. To do so, we derived a measure of mean-adjusted mRNA
137 expression noise[28], that accounts for dependence of mRNA expression noise on mean mRNA
138 expression, for 5475 genes from yeast single-cell RNA-seq data[40] (Fig. S3A,B). Overall, some of
139 the genes with low mean mRNA expression showed high mean-adjusted mRNA expression noise
140 (Fig. S3C). Next, we compared mRNA expression noise of the 16 classes of genes as obtained
141 based on the levels of mean mRNA expression and translational efficiency (Fig. 1B). The class of
142 genes with low mean mRNA expression and high translational efficiency showed the highest
143 mRNA noise among all classes (Fig. 1F). Specifically, this class of genes had significantly higher
144 mRNA noise (median mRNA noise = 0.068) compared to the class with high mRNA level and
145 low translational efficiency (median mRNA noise = -0.082; Mann-Whitney U-test, p=0.001, Fig.
146 1F). In general, mean-adjusted protein expression noise showed a moderate correlation with mean-
147 adjusted mRNA noise (Pearson's correlation = 0.44 and Spearman's correlation = 0.29, Fig. S3D).
148 These results suggested that high mRNA noise associated with low transcription, rather than the

low mean mRNA level itself, combined with translational efficiency was a good determinant of protein noise.

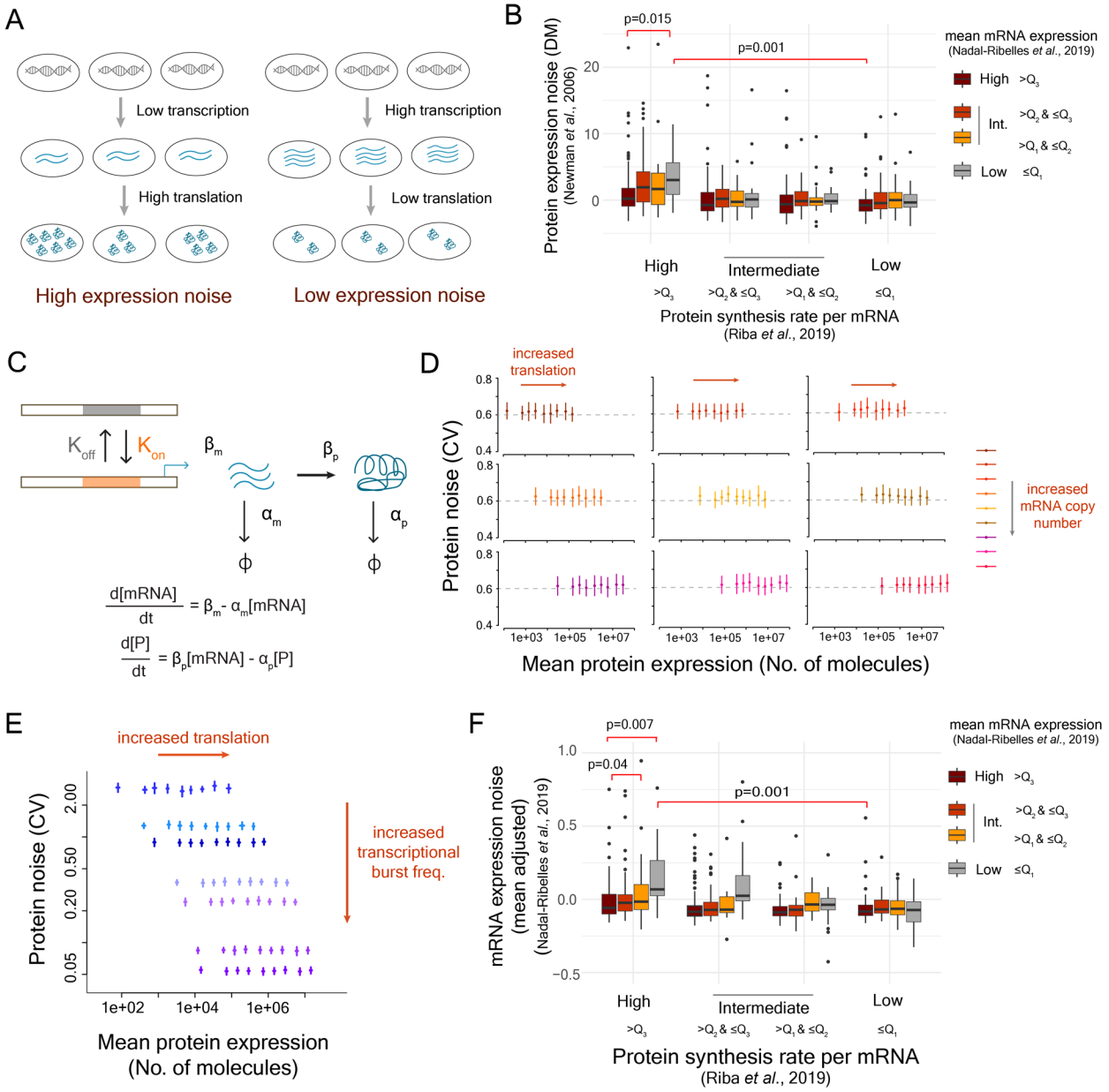

Fig. 1. High mRNA noise combined with high translational efficiency leads to high protein noise (A) Existing model describing the impact of translational efficiency on protein expression noise. **(B)** Genes were classified into 16 classes according to the quartiles of mean mRNA expression, calculated from Nadal-Ribelles *et al.*[40], and then by the quartiles of protein synthesis rates per mRNA from Riba *et al.*[41]. The protein noise values for genes in each of the classes were obtained from Newman et al. (2006), and the measure distance-to-median (DM) value, as derived in their work, was considered as the measure of noise. **(C)** Two-state model of gene expression

with the transition rates K_{on} and K_{off} between transcriptional ON and OFF states was used for stochastic simulations **(D-E)** Relationship between mean protein expression and protein noise (CV) obtained from stochastic modeling using the two-state model. The panel (D) describes the results of stochastic simulations obtained at different starting mRNA numbers of a gene to test whether the mRNA expression level of a gene can explain the positive relationship between mean protein expression and protein noise. The panel (E) shows the results obtained from stochastic simulations at different transcriptional burst frequencies, but keeping the starting mRNA number of the gene constant. **(F)** Mean-adjusted mRNA expression noise calculated from the single-cell RNA-seq data[40] in 16 classes of genes classified according to the quartiles of mean mRNA expression and the quartiles of translational efficiency based on the data on protein synthesis rate per mRNA from Riba *et al*., 2019[41]. Q_1, Q_2, and Q_3 represent first, second and third quartiles.

Bursty transcription combined with high translational efficiency leads to high protein noise

Based on the above observations, we put forward a new working model that highlighted the influence of mRNA noise in determining protein noise. Noise in mRNA expression is usually associated with bursty transcription, where low burst frequency leads to high mRNA expression noise and an increase in burst frequency gradually lowers mRNA noise as the transcription rate becomes more uniform. Therefore, we hypothesized that among genes that exhibited bursty transcription, the ones with high translational efficiency would show higher protein noise compared to the ones with low translational efficiency (Fig. 2A).

To test this new model, we estimated the parameters associated with transcriptional bursts such as on- and off- transition rates (K_{on} and K_{off}) and transcription rate (β_m) for >6000 genes in yeast from single-cell RNA-seq data[40] (Fig. S4), using a maximum-likelihood approach based on a Poisson-Beta model[44] (Fig. 2B). Genes with low transcriptional burst frequencies showed high mRNA noise (Fig. S5). However, the genes that exhibited high protein noise were associated with high translational efficiency (Fig. 2C). In addition, we classified genes into 16 classes according to the quartiles of burst frequency and the quartiles of translational efficiency[40] (Fig. 2D). Genes with low burst frequency and high translational efficiency showed the highest protein noise among all

16 classes (Fig. 2D). This class of genes showed a mean protein noise (DM) value of 5.65, whereas, the class of genes with high burst frequency and high translational efficiency showed a mean protein noise (DM) value of -0.038 (Mann-Whitney U test, $p=1.22 \times 10^{-7}$; Fig. 2D). These observations confirmed that high translational efficiency, combined with bursty transcription, could lead to high protein noise (Fig. 2D). Analysis with tAI as the measure of translational efficiency showed similar trend (Fig. S6, S7), suggesting that these results were robust to the use of different measures of translational efficiency.

Bursty translation does not explain the correlation between translational efficiency and protein noise

Even though results from the analysis of earlier experimental data agreed with the new working model, they did not explain how high translational efficiency combined with low burst frequency could lead to high protein noise, and how reducing translational efficiency could lower protein noise. Recent studies have observed that translation, like transcription, also occurs in bursts[38,39]. Specifically, Livingstone *et al.*[39], through single-cell mRNA tracking, measured the parameters of translational bursting and identified the roles of 5'UTR and 5'mRNA cap in modulation of translational burst frequency and burst amplitude.

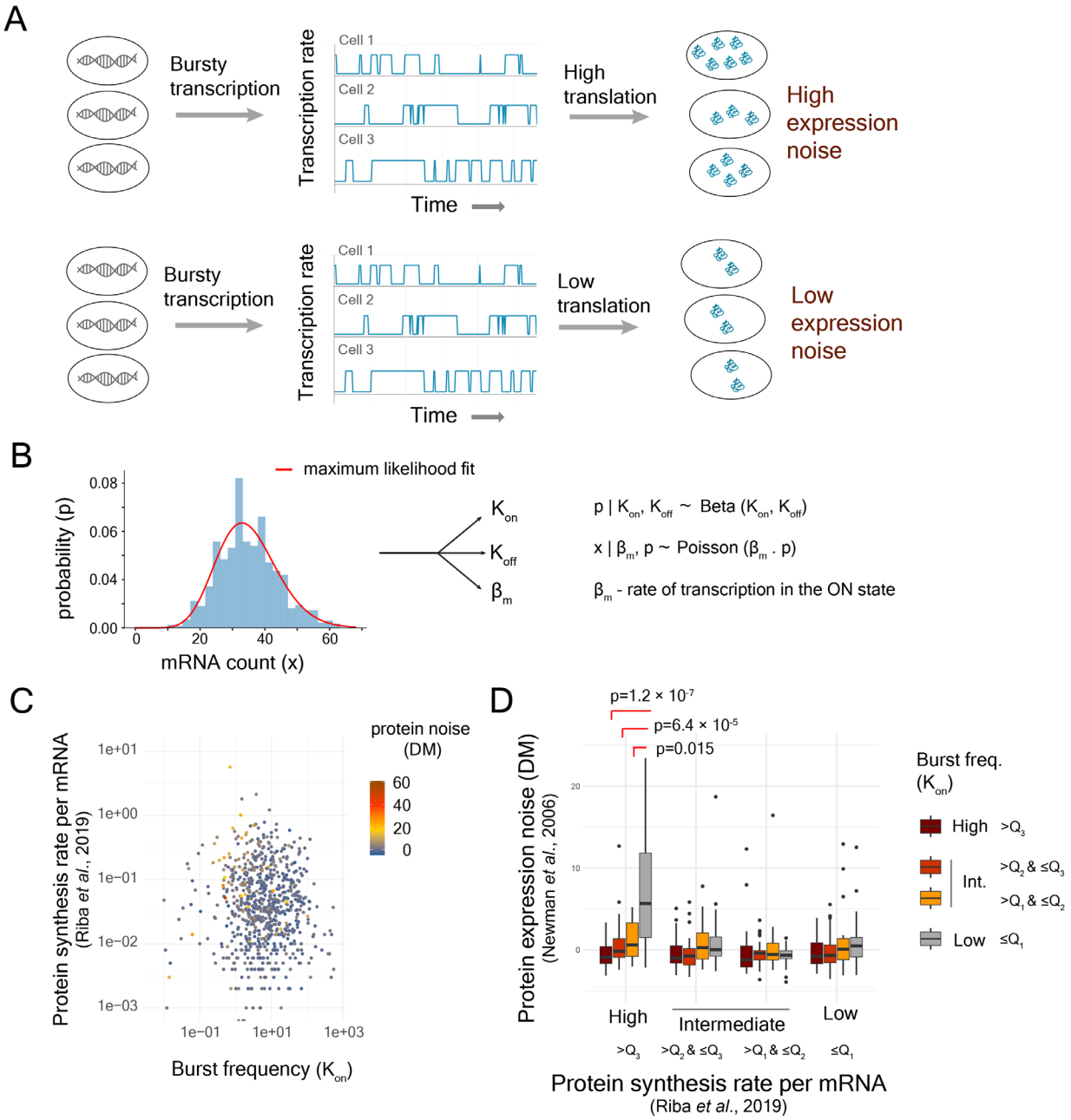

Fig. 2. Stochastic fluctuation in mRNA expression, originating from transcriptional bursts, combined with high translational efficiency generates high protein noise. (A) The new working model postulated that the genes with bursty transcription (low transcriptional burst frequency) and high translational efficiency were likely to exhibit higher protein expression noise compared to the genes with bursty transcription but low translational efficiency. **(B)** Estimation of parameters of two-state model of gene expression from single-cell RNA-seq data as described by Kim and Marioni (2013)[44]. **(C)** Protein noise of genes with different levels of transcriptional burst frequencies and translational efficiency, estimated by protein synthesis rates per mRNA[40]. **(D)** Protein expression noise (DM values from Newman *et al*., 2006) of genes classified into 16 classes

218 based on burst frequency and translational efficiency (protein synthesis rate per mRNA[41]). Q_1, Q_2,
219 and Q_3 represent first, second and third quartiles, respectively.
220

221

222 Therefore, we asked whether incorporating translational bursting into our model could reveal the
223 positive correlation between translational efficiency and protein noise. To do so, we built a TASEP
224 based model[45-46] of translation, with appropriate modifications, at the level of single mRNA
225 molecules (Fig. 3A, see Methods). We assumed that an mRNA molecule could transition between
226 on- and off-states[39] with the rates TL_{on} and TL_{off}, respectively, and in the on-state, translation
227 initiation occurred at the rate of TL_{init} (Fig. 3A). As multiple ribosomes could translate a single
228 mRNA molecule at the same time, a second translation initiation happened only when the
229 preceding ribosome traversed at least 10 codons, to account for steric interaction between
230 ribosomes[47,48] (Fig. 3B). Several earlier studies have showed the presence of a gradually increasing
231 profile of translational efficiency or ramp, although of different degree, in the 5' end of coding
232 regions of genes[34,49]. This meant that the translation speed was lower near the 5' end of a gene and
233 the speed gradually increased as a ribosome traversed from 5' to 3' end of an mRNA molecule.
234 Taking this into account, we modeled the traversal speed of the ribosomes using a first-order Hill
235 function where the traversal speed (V) was dependent on the position of the ribosome in the coding
236 sequence (Eq. 10; Fig. 3B). An increase in the value of the parameter K_{Hill} led to an increased
237 traversal time (Fig. 3C). The speed of traversal has an impact on translation initiation rate, as
238 observed by Barrington *et al.*[50]. This meant that K_{Hill} was also related to the translation initiation
239 rate, TL_{init}. Higher translation initiation rate necessitated lower K_{Hill} to ensure faster traversal of
240 the preceding ribosome through first 10 codons to avoid collision between two successive
241 ribosomes (Fig. 3D). Similarly, lower K_{Hill} value led to faster traversal of ribosomes through an
242 mRNA molecule, and thereby, permitted a greater number of translation initiation events per unit

243 time (Fig. 3D). Thus, the translation initiation rate and the ribosome traversal time through an

244 mRNA molecule were interconnected (Fig. 3D).

245

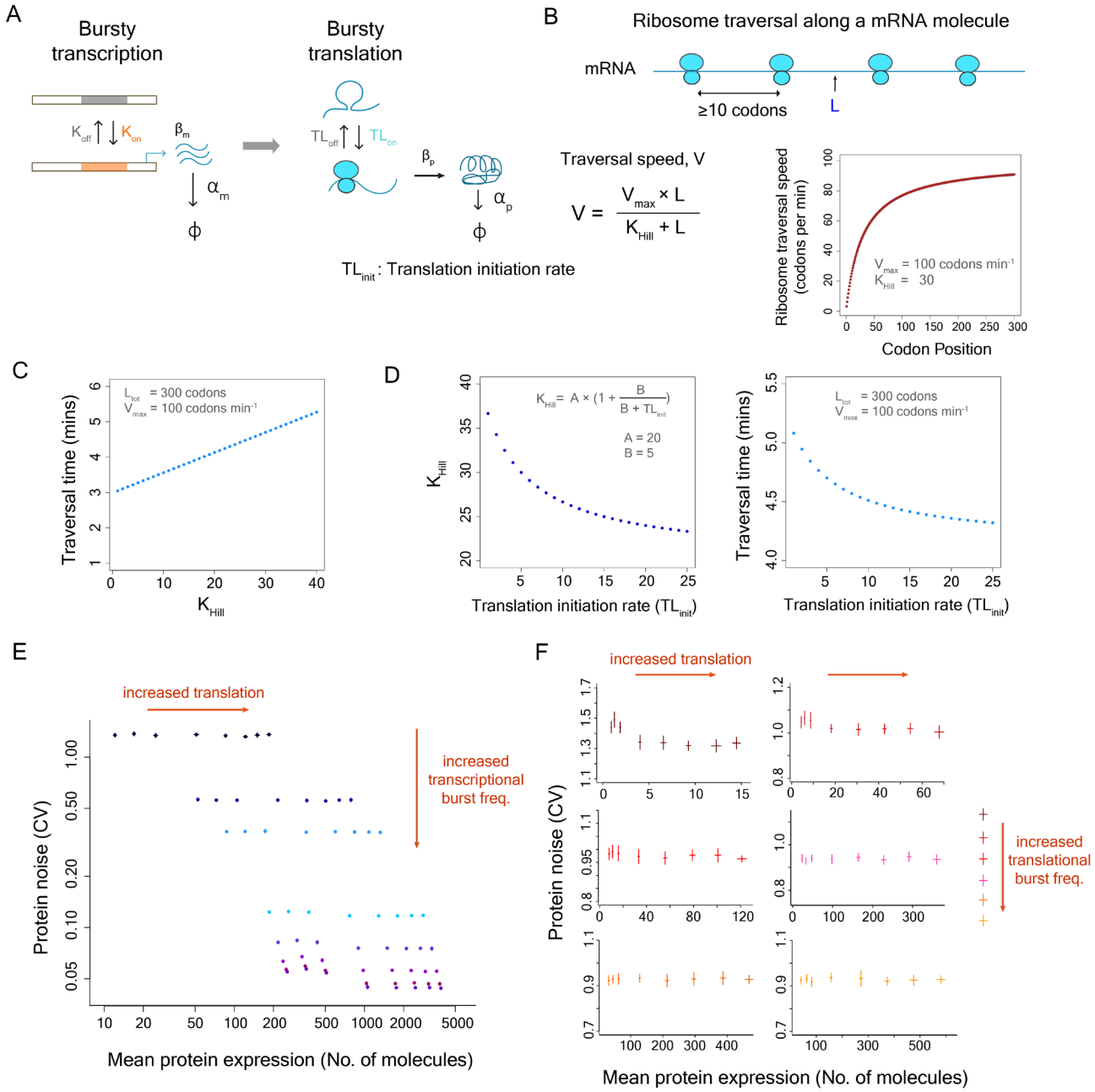

246

247 **Fig. 3. The model combining transcriptional and translational bursting does not explain the**
248 **positive correlation between translational efficiency and protein noise (A)** Schematic diagram
249 depicting the integrated model of transcriptional and translational bursting. **(B)** Ribosomal

traversal speed along an mRNA molecule is given by V at a position L in the mRNA molecule. As multiple ribosomes could translate a single mRNA molecule at the same time, a second translation initiation happened only when the preceding ribosome traversed at least 10 codons, to account for steric interaction between ribosomes[47,48]. The ribosome traversal speed was modeled using a Hill function as several studies have shown the presence of a gradually increasing profile of translational efficiency or ramp in the 5' end of coding regions of genes[34,49] **(C)** Traversal time calculated as a function of K_{Hill} from the Hill function for a gene with 300 codons, and the maximum traversal speed of 100 codons per minute. **(D)** Relationship between K_{Hill}, translation initiation rate and ribosome traversal time. Faster ribosome traversal enabled higher translation initiation rate (TL_{init})[50]. A and B are parameters of the model. **(E)** The results obtained from stochastic simulations using the combined model of transcriptional and translational bursting. Protein noise changes with changes in translational efficiency and transcriptional burst frequency, but do not reveal a positive correlation between mean protein expression and protein noise **(F)** Protein noise obtained from the combined model changes with changes in translation initiation rate and translational burst frequency, but do not explain the positive correlation between mean protein expression and protein noise.

We integrated the model of translation with the two-state model of transcription, and performed stochastic simulations in individually in 1000 cells to estimate mean protein expression and protein noise (coefficient of variation, CV). To test whether incorporation of the translational bursting could capture the positive correlation between mean protein expression and protein noise, we changed the translational efficiency by varying the translation initiation rate (TL_{init}) in our simulations, thereby, also affecting the ribosome traversal time, while keeping all other parameters constant. For all transcriptional burst frequencies examined, we did not observe any change in protein noise with an increase in translational efficiency (Fig. 3E). We also tested the model at different translational burst frequencies. Although changes in translational burst frequencies altered the level of protein noise, we did not find any correlation between mean protein expression and protein noise (Fig. 3F). These results suggested that a simple model integrating transcriptional and translational bursting could not explain the observed relationship between translational efficiency and protein noise.

281 **Inclusion of ribosome demand reveals a positive correlation between translational efficiency**
282 **and protein noise**

283 Next, we analyzed several molecular models that could possibly explain the positive correlation
284 between translational efficiency and protein noise. An increase in translational efficiency, leading
285 to a higher translation rate, will require an increased supply of tRNA molecules and ribosomes.
286 Could an increase in translation rate lead to a bottleneck in supply of tRNA, and generate variation
287 in protein expression across cells? This seemed highly unlikely, as high translational efficiency is
288 associated with presence of preferred codons, for which abundant tRNA molecules are available
289 in a cell[33,34]. In comparison, rare codons have lower numbers of corresponding tRNA molecules
290 available[33,34]. Thus, presence of rare codons would, in fact, cause a bottleneck in tRNA supply and
291 hence, would lead to higher expression noise. This would further imply that a reduction in
292 translational efficiency would generate higher expression noise, which would contradict the actual
293 empirical observations[30,31].
294

295 The translational efficiency is dependent on availability of ribosome machinery in the cell. We
296 analyzed whether higher translational efficiency could lead to a bottleneck in the availability of
297 ribosomes for mRNA molecules of a gene, cause variation in the translation process of a gene
298 among cells and thereby, generate high expression noise. It has been reported that competition for
299 ribosomes rather than tRNA, imposes constraints on translation in yeast[51]. In addition, studies in
300 cell-free systems have shown that constraints on resources for transcription and translation can
301 cause bursty expression[52].

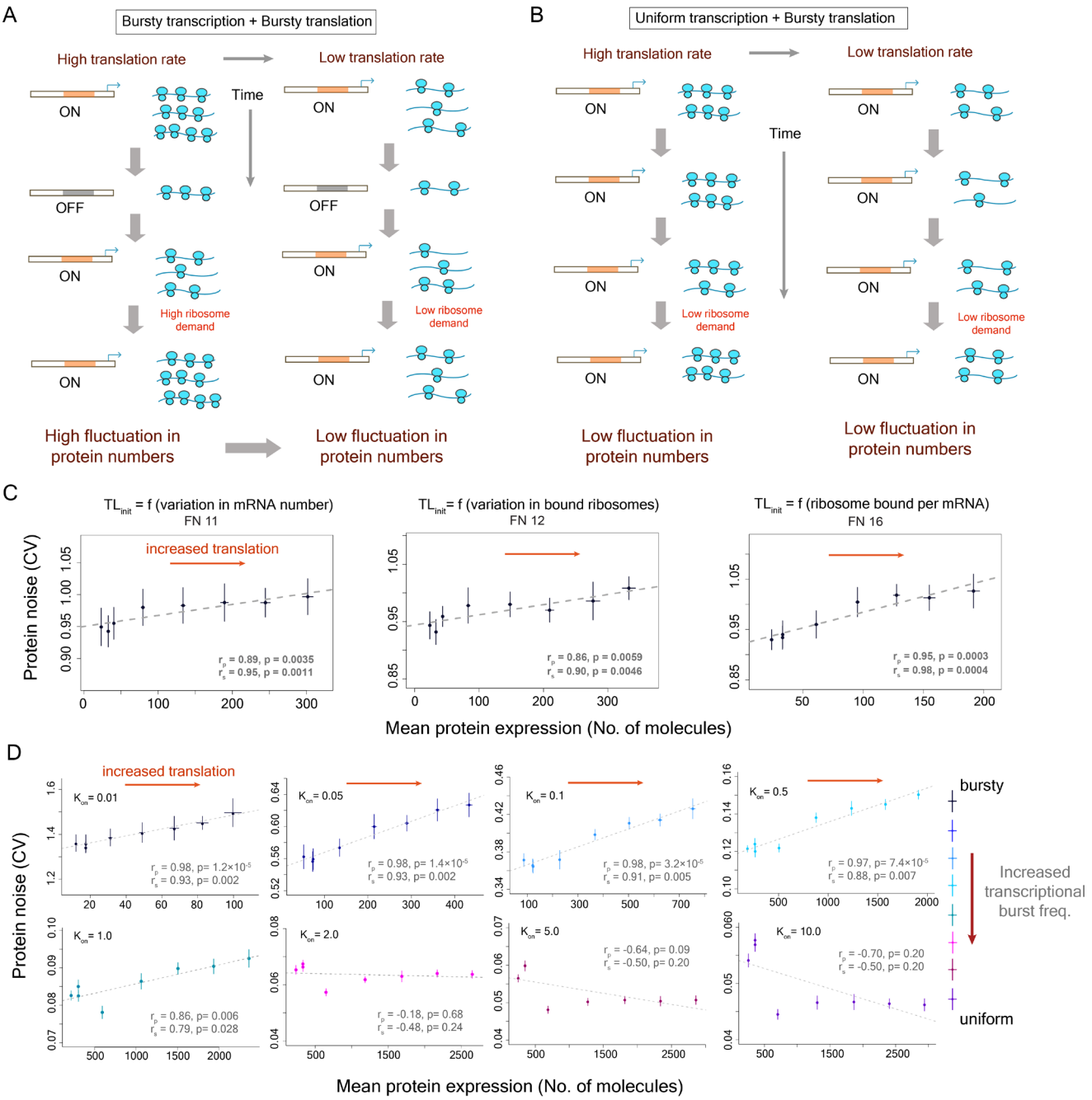

Fig. 4. Inclusion of ribosome demand associated with translation of mRNA molecules of a gene can reveal positive correlation between translational efficiency and protein noise (A) Schematic diagram depicting how ribosome demand for translation of mRNA molecules can vary with bursty transcription and bursty translation. As mRNA numbers of the gene fluctuate due to bursty transcription, high translational efficiency can lead to intermittent elevated ribosome demand for translation of the mRNA molecules of that gene. This can lead to increased inter-individual variation in protein numbers **(B)** Uniform transcription of a gene does not lead to a sudden elevated ribosome demand for translation, thereby reducing inter-individual variation in protein numbers **(C)** Results from simulations with three different functions (function 11, 12 and

16 from Table S1) that model the impact of ribosome demand on translational efficiency. Results from simulations with other functions to model ribosome demand are shown in Fig. S8. **(D)** The relationship between mean protein expression and protein noise at different transcriptional burst frequencies obtained from stochastic simulations with the model incorporating ribosome demand along with transcriptional and translational bursting. The ribosome demand was modeled using function 16 (Table S1). For each transcriptional burst frequency, the translational efficiency was altered by changing the translation initiation rate (TL_{init}) while keeping rest of the parameters constant.

For a gene that is transcribed in bursts, there will be considerable temporal fluctuation in the number of mRNA molecules available for translation. When the mRNA copy number of that gene is high, they will require many ribosomes for translation. As the mRNA copy number drops due to stochastic fluctuations in transcription rate, some of the ribosomes earlier involved in translation of mRNA molecules of this gene become available, and can be allocated for translating mRNA molecules of other genes (Fig. 4A). At a subsequent time-point when the mRNA number of this gene rises again, it increases the demand for ribosomes (Fig. 4A). In actively growing cells, where the demand for ribosomal machinery is high, this can constrain translation initiation rate for these mRNA molecules. As the allocation of ribosomes to mRNA molecules is likely to be a stochastic process, this can generate variation in translation rates and consequently, protein expression of that gene between cells.

There are two predictions that come out of this model. First, it predicts that a reduction in the high demand for ribosome machinery during the low- to high- mRNA copy-number transition will lower protein expression noise (Fig. 4A). This can be achieved by lowering the translational efficiency of the gene. In this scenario, we will observe high protein noise at high translational

338 efficiency and low noise at low translational efficiency, which will agree with the empirical
339 observations.
340
341 Another way of minimizing the sudden demand for ribosomes is to reduce temporal fluctuations
342 in mRNA numbers. This can be achieved at the level of transcription by employing a more uniform
343 rate of transcription (Fig. 4B). Thus, according to the second prediction, protein noise of genes
344 that are expressed in a uniform rate of transcription will be minimally affected by changes in the
345 translational efficiency (Fig. 4B).
346
347 In addition, we explored whether co-translational protein folding, ribosome collision, translational
348 errors, or changes in mRNA stability associated with translation rate could explain the positive
349 association between translational efficiency and protein noise. Proteins are co-translationally
350 folded as they exit through the ribosome tunnel after translation[53]. The speed of translation might
351 affect the efficiency of co-translational folding, and perhaps, fast translation could lower efficiency
352 of co-translational folding. This can generate misfolded proteins that are degraded. Since this
353 process is stochastic in nature, it can lead to increased variation in protein expression among cells
354 within a population. However, several studies have reported the exactly opposite phenomenon. A
355 study by Spencer *et al.*[54] showed that the use of optimal codons leads to better folding of the
356 encoded polypeptide. Other studies have shown that fast translation can in fact help avoid
357 misfolded states, and can help in better co-translational folding, especially for misfolding-prone
358 regions[55,56].
359
360 High translational efficiency means fast traversal of ribosomes through an mRNA molecule which
361 would in turn increase the translation initiation rate. This can lead to a higher chance of collision

362 between two successive ribosomes on an mRNA molecule in case of a slow-down in movement
363 due to occurrence of non-preferred codons. Slower ribosome traversal reduces translation initiation
364 rate and thus, lowers the chance of ribosome collision even in case of a slow-down. Ribosome
365 collision leads to degradation of mRNA, rescue of bound ribosome and can also affect further
366 translation initiation[57-59]. Therefore, this could be a possible reason for higher protein noise in
367 genes that show high translational efficiency. However, in contrast to the ribosome demand model,
368 this observation would hold for all genes with high translational efficiency, irrespective of their
369 burst frequencies.
370
371 We further considered whether translational errors could explain the correlation between
372 translation rate and protein expression noise. It is possible that fast translation can lead to more
373 translational errors. This can generate proteins with wrong amino acids, which can result in protein
374 misfolding and therefore, can lead to protein degradation. Since translational errors occur at
375 random, this process will vary from one cell to another, which can lead to higher protein expression
376 noise. However, there are conflicting reports regarding this. An earlier study reported that
377 translational errors occurred at sites where the speed of ribosome was higher[60]. On the other hand,
378 a recent study observed that preferred or optimal synonymous codons, where ribosome traversal
379 is fast, were translated more accurately[61].
380
381 Finally, we also considered whether the translation process itself could change mRNA stability
382 and therefore, could generate cell-to-cell variation. It has been reported that increased translation
383 can lead to higher mRNA destabilization[62]. In addition, codon optimality and thus elongation rate
384 has also been suggested to be positively associated with mRNA stability[63]. A more recent study
385 has however showed that translation initiation rate, but not elongation rate, is the major

386 determinant of mRNA stability and inhibition of translation initiation has been shown to increase
387 mRNA decay[64]. However, if changes in the translation rates altered mRNA stability and led to
388 increased variation in cell-to-cell variation in protein concentration, this will be observed for all
389 genes irrespective of their burst characteristics.
390
391 Since the ribosome demand model agreed with the earlier empirical observations, we tested
392 whether incorporating ribosome demand in our mathematical model could capture the observed
393 positive correlation between translational efficiency and protein noise. The ribosome demand for
394 translating the mRNA molecules of a specific gene was modeled as a resource allocation problem
395 that depended on the fluctuation in the number of mRNA molecules of that gene and the number
396 of ribosomes that were available for translation of these mRNA molecules (Fig. 4A). Large
397 variation in mRNA numbers led to large fluctuations in ribosome demand which also affected
398 translation initiation rate. For example, a sudden surge in the number of mRNA molecules of the
399 gene from one time point to another necessitated more ribosomes for translation, thereby, creating
400 increased ribosome demand for translation of that gene. Similarly, large variation in the number
401 of ribosomes required to be bound to mRNA molecules of that gene between two consecutive time
402 points affected ribosome allocation and influenced translation initiation rate.
403
404 Therefore, we modeled ribosome demand using various mathematical functions (Table S1) where
405 we considered it to be a function of variation in mRNA number, variation in ribosome bound per
406 mRNA molecule or a combination of both (the parameter 'av', Table S1). The translation initiation
407 rate (TL_{init}) at a specific time point varied from the basal translation initiation rate according to
408 Hill functions incorporating ribosome demand (Table S1). The Hill functions were of the order 10
409 to model a sharp decrease in translation initiation rate if the ribosome demand was too high. For

410 each of the functions for modeling ribosome demand, we performed stochastic simulations and
411 changed mean expression by varying the basal translation initiation rate while keeping other
412 parameters constant (Fig. 4C, Fig. S8).
413
414 Interestingly, the functions where translation initiation rate was dependent on the number of
415 ribosomes bound per mRNA molecule showed the most positive association between mean protein
416 expression and protein noise (Fig. 4C, Fig. S8). We, therefore, considered one of these functions
417 (function 16) for all subsequent analysis (Fig. 4C, Table S1). However, we observed similar
418 positive association for several variants of these functions suggesting that the association found
419 was robust to variations in the actual form of the function (Table S1, Fig. S8).
420
421
422 To further test whether our mathematical model could capture the two predictions of the ribosome
423 demand model, we performed stochastic simulations for a wide range of transcriptional and
424 translational burst frequencies (Fig. 4D). At low transcriptional burst frequencies, protein noise
425 increased with an increase in translation rate (Fig. 4D). In addition, as we increased the
426 transcriptional burst frequency and moved towards a more uniform rate of transcription, the
427 translation rate had minimal effect on protein noise (Fig. 4D). Thus, the mathematical model could
428 recapitulate both predictions of the ribosome demand model.
429
430
431
432
433
434
435
436

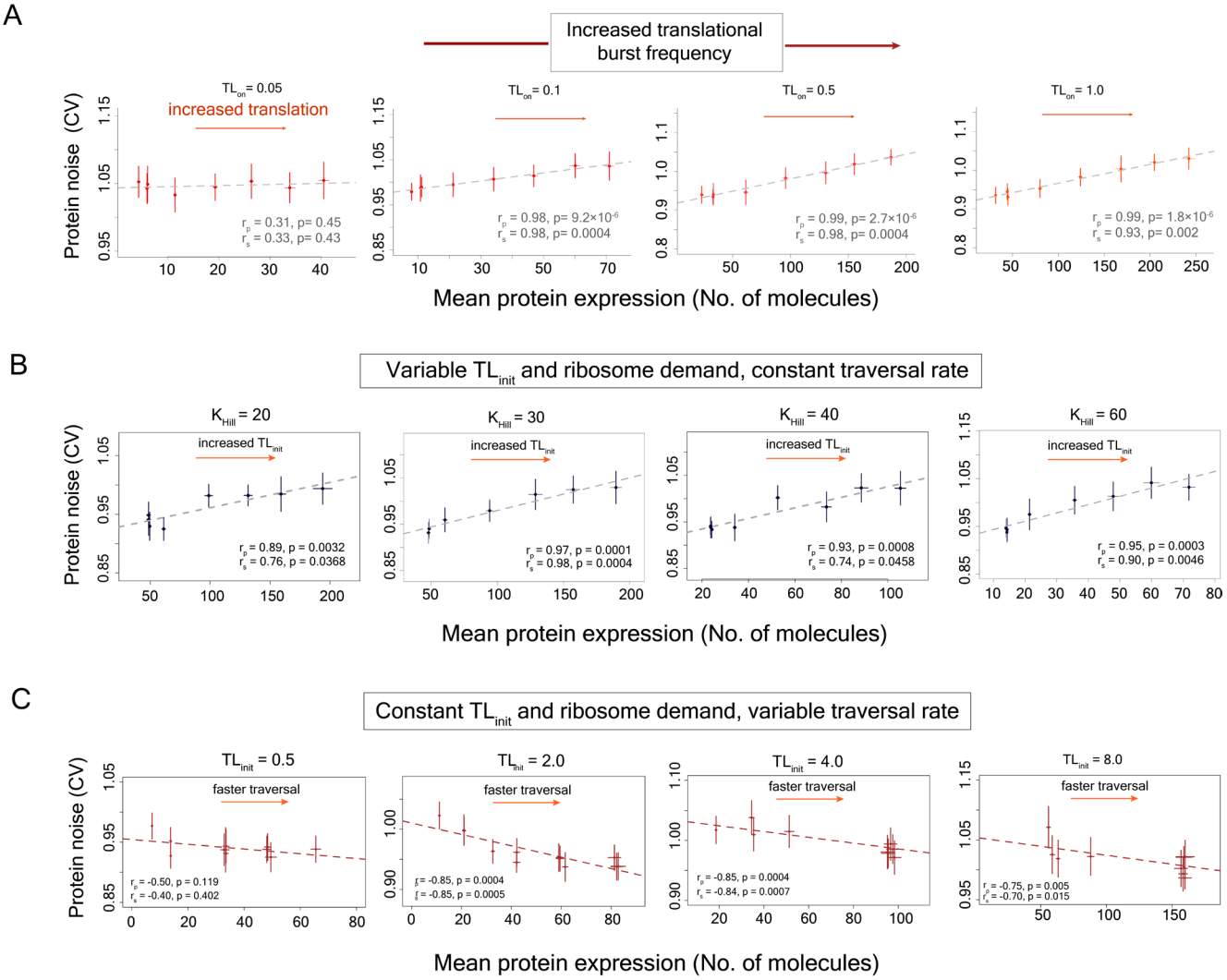

Figure 5 – Ribosome demand is necessary for the positive correlation between mean protein expression and protein noise. (A) The relationship between mean protein expression and protein noise at different translational burst frequencies obtained from stochastic simulations with the model incorporating ribosome demand along with transcriptional and translational bursting. The ribosome demand was modeled using function 16 (Table S1). For each transcriptional burst frequency, the translational efficiency was altered by changing the translation initiation rate (TL_{init}) while rest of the parameters were kept constant. **(B)** Stochastic simulations where mean protein expression was altered by changing base translation initiation rate (TL_{init}), thus altering ribosome demand, but keeping ribosome traversal speed constant, maintained positive correlation between mean protein expression and noise. This was done by keeping K_{Hill} constant at specific values during simulations that constrained the traversal time (Eq. 10). **(C)** Stochastic simulations where mean protein expression was altered by changing the ribosome traversal speed (Eq. 10) but keeping the base translation initiation rate (TL_{init}) constant, and thus, not allowing variation in ribosome

demand with changes in ribosome traversal rate, abolished the positive correlation between mean protein expression and protein noise.

We also tested the impact of translational burst frequency on the association between translational efficiency and protein noise (Fig. 5A). At very low translational burst frequencies, protein noise did not show much change with an increase in translation rate (Fig. 5A). This was due to very low level of protein production at very low translational burst frequency, as mRNA molecule mostly resided in the inactive state. At higher translational burst frequencies, we again observed an increase in protein noise with an increase in the translation rate and hence with an increase in mean protein expression (Fig. 5A). We further tested the robustness of our stochastic modeling approach through a systematic variation in values of several model parameters (Fig. S9-S14), as well as explored different scenarios through random sampling of the parameter space (Fig. S15).

Next, we investigated whether elimination of the ribosome demand from our model could lead to a loss of the positive correlation between mean protein expression and protein noise. To do so, we tested two sets of models where we decoupled the translation initiation rate (TL_{init}) from the ribosome traversal speed (V) and changed each of these parameters independently without varying the other. In the first set of models and stochastic simulations, we altered the mean protein expression of the gene by altering the base translation initiation rate but keeping the ribosome traversal speed constant. In these models, ribosome demand varied with changes in the basal translation initiation rate and maintained the positive correlation between mean protein expression and protein noise (Fig. 5B). The results were similar for ribosome traversal speed set at different values defined by the Hill coefficient (K_{Hill}) according to the equation 10. In the second set of models and simulations, we changed the mean protein expression by altering the ribosome traversal speed but keeping the translation initiation rate constant. These models did not allow

477 ribosome demand to vary according to the changes in the ribosome traversal speed and showed a
478 loss of positive correlation between mean protein expression and protein noise (Fig. 5C and S16).
479 Thus, these results suggested that the ribosome demand was necessary for maintaining the positive
480 correlation between mean protein expression and protein noise.
481
482
483 **Impact of coding sequence mutations on protein noise is dependent on the burst**
484 **characteristics of the promoter**
485 To empirically test the predictions of the ribosome demand model, we set up an experimental assay
486 to measure protein expression noise in the yeast model system (Fig. 6A). We built gene constructs
487 where the expression of a green fluorescent protein (*GFP*) gene could be controlled by different
488 promoters with different burst frequencies (Fig. S17). We then introduced several mutant variants
489 of the GFP gene with altered translational efficiencies, under the regulation of these promoters.
490 We integrated all constructs into the yeast genome, to eliminate expression noise arising from
491 fluctuations in plasmid copy number (Fig. 6A). We measured GFP expression using flow
492 cytometry (Fig. S18), and estimated noise from a homogeneous group of cells that showed very
493 similar cell size and cell complexity[14] (Fig.6B, Fig. S19).
494
495 We picked four promoters for our constructs (Fig. 6C) - two promoters, of *RPG1* and *RPL35A*
496 genes, with high burst frequencies (K_{on}=22.855 and K_{on}=47.464 respectively) and low protein
497 noise (DM=-0.841 and DM=-1.4 respectively)[15], and two promoters, of *CPA2* and *QCR2* genes,
498 with low burst frequencies (K_{on}=0.704 and K_{on}=1.186 respectively) and high protein noise
499 (DM=9.583 and DM=3.515 respectively)[15]. Our measurements also confirmed that the promoters
500 *CPA2* and *QCR2* had higher protein noise compared to *RPG1* and *RPL35A* (Fig. 6D).

501

502 To change translational efficiency in all gene constructs in a similar manner, we built variants of
503 the GFP gene that differed in their codon usage. This altered the translation elongation rate which
504 in turn would also alter the translation initiation rate[50]. We constructed nine mutant variants of the
505 *GFP* gene and cloned each of them under the control of these four promoters. The variants
506 consisted of seven single mutants and two variants with multiple mutations (see Methods). Many
507 of the codon substitutions led to usage of nonpreferred codons in yeast. We specifically focused
508 on mutating N-terminal and C-terminal regions of the GFP protein so as not to affect its functional
509 core. In addition, variants contained mostly synonymous mutations with two exceptions. We
510 changed glutamic acids with aspartic acids at codon 5 and codon 234, and tyrosine with asparagine
511 at codon 237 of the GFP gene. We created all constructs in three replicates, and estimated their
512 noise through multiple independent experiments on different days.

513

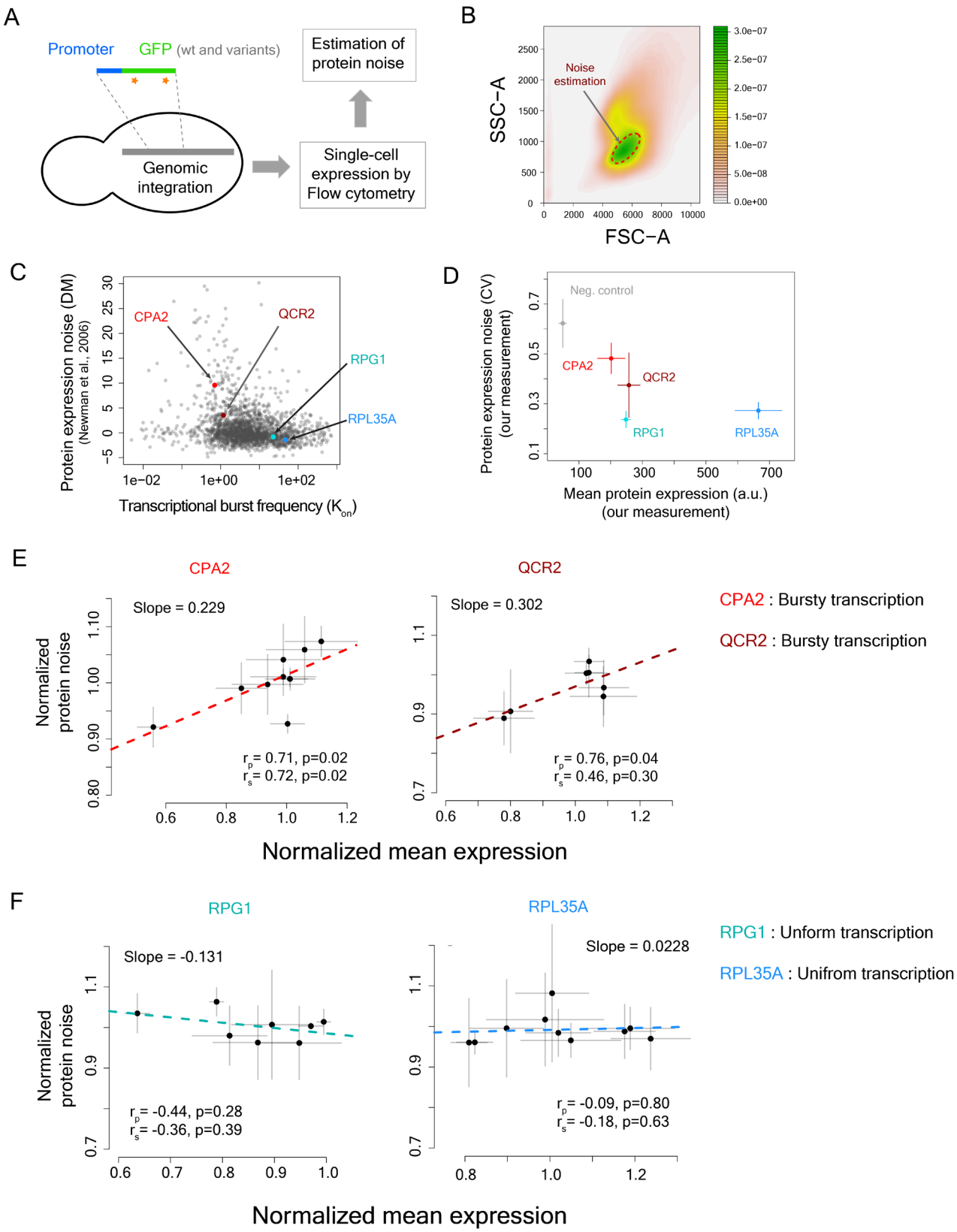
A
Promoter
GFP (wt and variants)
Genomic integration
Single-cell expression by Flow cytometry
Estimation of protein noise
B
Noise estimation
SSC−A
FSC−A
C
CPA2
QCR2
RPG1
RPL35A
Protein expression noise (DM)
(Newman et al., 2006)
Transcriptional burst frequency (K_on)
D
Neg. control
CPA2
QCR2
RPG1
RPL35A
Protein expression noise (CV)
(our measurement)
Mean protein expression (a.u.)
(our measurement)
E
CPA2
QCR2
Slope = 0.229
Slope = 0.302
r_p = 0.71, p=0.02
r_s = 0.72, p=0.02
r_p = 0.76, p=0.04
r_s = 0.46, p=0.30
Normalized protein noise
Normalized mean expression
CPA2 : Bursty transcription
QCR2 : Bursty transcription
F
RPG1
RPL35A
Slope = -0.131
Slope = 0.0228
r_p = -0.44, p=0.28
r_s = -0.36, p=0.39
r_p = -0.09, p=0.80
r_s = -0.18, p=0.63
Normalized protein noise
Normalized mean expression
RPG1 : Unform transcription
RPL35A : Unifrom transcription

514

515

516
517 **Fig. 6. Impact of changes in translational efficiency on protein noise is dependent on the**
518 **transcriptional burst characteristics of promoters (A)** Gene-promoter construct for genomic
519 integration and noise measurement **(B)** Noise estimation from a homogeneous group of cells with
520 similar cell size and complexity **(C)** Protein noise (DM)[15] vs burst frequency values for yeast
521 genes. Burst frequency values were estimated from single-cell RNA-seq data[40] using the method
522 described by Kim and Marioni (2013)[44]. **(D)** Measured mean protein expression and protein noise
523 of the promoters of *RPL35A*, *RPG1*, *CPA2* and *QCR2* with the wild-type GFP gene. **(E)**
524 Relationship between normalized protein noise and normalized mean expression of the GFP
525 mutants in the bursty promoters *CPA2* and *QCR2*. (F) Relationship between normalized protein
526 noise and normalized mean expression of the GFP mutants in the non-bursty promoters *RPG1* and
527 *RPL35A*.
528
529
530 The multi-mutant variant at the N-terminal end, containing five mutations (N-5), had the most
531 number of rare codons and thus, was expected to show substantial reduction in mean protein
532 expression owing to its low translational efficiency. We compared the impact of the coding region
533 mutations across different promoters through the measures of normalized mean expression and
534 normalized protein noise (Fig. S20A,B), to account for differences in mean protein expression and
535 absolute protein noise among the four promoters. The N-terminal multi-mutant (N-5) showed
536 substantial reduction in normalized mean protein expression (~56-81% mean expression compared
537 to the wild-type GFP gene) across all promoters (Fig. S20A). Very interestingly, the N-5 mutant
538 also showed substantial reduction in protein noise values, but only when expressed under the
539 bursty promoters *CPA2* and *QCR2* (Fig. S20B). This mutant showed 8% and 11 % reduction in
540 normalized protein noise compared to the wild-type GFP gene when expressed under the *CPA2*
541 and *QCR2* promoters respectively (Mann-Whitney U test, $p=1.2\times10^{-4}$ and $p=6.7\times10^{-4}$
542 respectively), but showed much lower change in normalized protein noise when expressed under
543 the regulation of the promoters *RPG1* and *RPL35A* (~3% increase and ~4% decrease in CV
544 respectively) (Fig. S20B), despite 36% and 19% decrease in mean expression under the regulation
545 of these non-bursty promoters.

546

547

548 Analysis of the relationship between normalized protein noise and normalized mean expression
549 across all GFP variants revealed very interesting results. The regression line fitted to the plot of
550 normalized mean protein expression against normalized protein noise showed positive slopes only
551 for bursty promoters *CPA2* and *QCR2* (slope of 0.229 and 0.302 respectively, Fig. 6E), like what
552 had been observed before[30,31]. In contrast, the regression line for the promoters *RPL35A* and *RPG1*
553 showed near-zero or negative slope (Slope of -0.131 and 0.0228, respectively, Fig. 6F). Genome-
554 wide analysis of relationship between protein noise and protein synthesis rate per mRNA or tAI
555 for groups of genes with different transcriptional burst frequencies also showed similar trend, with
556 stronger positive relationship between protein noise and translational efficiency for genes with
557 bursty transcription ($K_{on} \leq Q_1$, first quartile of burst frequency) (Fig. S21). These results were in
558 line with the predictions from stochastic simulations, and therefore, suggested that variation in
559 ribosome demand was indeed the molecular link between stochastic fluctuations in mRNA
560 numbers and protein noise.

561

562

563 **Discussion**

564 Taken together, our work provides unique molecular insights into the long-standing observation
565 of positive correlation between translational efficiency and protein noise. We test the long-held
566 assumption that low transcription rate combined with high translational efficiency can generate
567 this positive correlation. We show that the high protein noise in genes with low transcription rate
568 and high translational efficiency primarily stems from higher stochastic variation in mRNA
569 numbers associated with low rate of transcription. We also show that demand for ribosomal

570 machinery underlies translational modulation of transcriptional noise. Thus, our work reveals how
571 the coding sequences of genes can influence expression noise, and how this contribution is
572 dependent on the properties of the promoter. This work also highlights how dynamic properties of
573 a system and shared resources influence gene expression, beyond genetic features such as promoter
574 sequence or presence of specific motifs.
575
576 Our results also illustrate how the translation process can decouple mean protein expression and
577 protein noise[27], with a departure from the traditional inverse relationship between them. The nature
578 and extent of translational decoupling is dictated by the translational efficiency of the coding
579 sequence, as well as by the promoter and its mode of transcription.
580
581 There are several other factors besides codon usage that can impact translational efficiency. For
582 example, presence of micro-ORF upstream of the start codon and presence of mRNA secondary
583 structures in the 5' UTR region can affect translational efficiency [35,65]. In addition, presence of a
584 stretch of positively- charged residues in the amino acid chain can slow down movement of the
585 growing peptide chain through the ribosomal exit tunnel and can impact translational efficiency
586 [66]. Thus, the effective translational efficiency for a gene is a complex combination of multiple
587 variables. It remains to be seen how these variables combine with translational bursts and impact
588 expression noise.
589
590 In summary, our work identifies variation in ribosome availability as the key feature driving the
591 translational modulation of transcriptional bursts. Such variation happens across organisms and
592 therefore, these results have broad implications for studying protein noise across biological
593 systems. Advancements in single-cell RNA sequencing have enabled us to study mRNA

594 expression noise across diverse cellular processes in different organisms. However, noise at the
595 protein level has more direct impact on cellular phenotypes and therefore, on phenotypic
596 heterogeneity. Thus, a better understanding of how mRNA noise is linked to protein noise will
597 help us better predict phenotypic heterogeneity. Our work further shows that combining estimates
598 of burst parameters from single-cell RNA-sequencing data with tAI values of genes can help
599 predict protein expression noise. As more single-cell RNA-seq data become available, this will
600 greatly facilitate estimation of protein expression noise, and will enhance our understanding of its
601 impact on cellular processes across different biological systems.
602

603 ## Materials and Methods

604 **Datasets**

605 The mean mRNA expression levels of yeast genes were calculated from the single-cell RNA-seq
606 data in yeast[40]. Mean mRNA expression values for 5500 genes were obtained from this data. Noise
607 in mRNA expression was calculated following the method described in Parab *et al*.[28]. Briefly, for
608 each gene, mean expression, standard deviation and subsequently, coefficient of variation (CV)
609 values were calculated. In the next step, polynomial functions of different degrees were fitted to
610 the CV vs log-transformed mean mRNA expression plot, and the best fit was chosen. The
611 polynomial function of order 5 was observed to give the best fit and was used for calculating mean-
612 adjusted mRNA expression noise. For each gene, mean-adjusted mRNA noise was calculated by
613 the distance of the vertical line drawn from its CV value to the fitted spline. Protein expression
614 noise values for genes were obtained from Newman *et al.*[15] and their Distance-to-Median (DM)
615 values, that were corrected for dependence of CV on mean protein expression, in YPD medium
616 were used. Protein noise of 2763 genes were obtained from this data. For translational efficiency,

617 the data from Riba *et al.*[41] were used, and for each gene, the real protein synthesis rate per mRNA
618 value from their data was considered as its measure of translational efficiency. The tAI values for
619 all yeast genes were calculated using tAI value of each codon in yeast from Sabi *et al.*[67], according
620 to the method described in Tuller *et al.*[34].
621
622 **Two-state model for bursty transcription**
623 Transcriptional bursts were modeled using a two-state model where a gene transitioned between
624 on- and off- states[42]. The rate of transitions to on- and off- states were considered to follow Poisson
625 distributions individually and thus, the time intervals between two on-transitions or off-transitions
626 were exponentially distributed. The time intervals between successive events (on- or off-
627 switching) were sampled from exponential distributions with rate parameters K_{on} and K_{off}
628 respectively. Transitions to on-state resulted in production of mRNA at a rate β_m and translation of
629 these mRNA molecules to proteins at a rate β_p. These mRNA and protein molecules were
630 considered to undergo removal, resulting from dilution due to cell growth and degradation, at the
631 rates of α_m and α_p respectively.
632
633 The dynamics of transcription and translation were modeled using the following equations.
634 $Change\ in\ mRNA\ conc.\ over\ time$: $\frac{d[mRNA]}{dt} = \beta_m - \alpha_m \times [\text{mRNA}]$ …… (Eq. 1)
635 where β_m denoted the transcription rate per unit time (or burst size) and α_m denoted the removal
636 rate of mRNA due to degradation and dilution.
637 Similarly, $Change\ in\ protein\ conc.\ over\ time$: $\frac{d[P]}{dt} = \beta_p \times [\text{mRNA}] - \alpha_p[\text{P}]$ …… (Eq. 2)
638 where β_p denoted the protein production rate from mRNA and α_p denoted the protein removal rate.
639

640 Stochastic simulations were performed using Gillespie's algorithm[43] to model changes in the
641 numbers of mRNA and protein molecules over time. The behavior of the system was tracked at
642 small discrete time intervals Δt from the initial time point t. These resulted in observations at 'n+1'
643 time points t, t+ Δt, t+2×Δt, …, t+n×Δt. Any event of binding or unbinding occurring within a time
644 interval was noted and resulted in changes in transcription rate which eventually led to a change
645 in protein concentration. As the time interval Δt was small, the equations modeling the behavior
646 of the systems was simplified as

647 $$[mRNA]_{t+\Delta t} = [mRNA]_t + (\beta_m - \alpha_m \times [mRNA]_t) \times \Delta t \quad \text{…… (Eq. 3)}$$

648 and $$[P]_{t+\Delta t} = [P]_t + (\beta_p \times [mRNA]_t - \alpha_p \times [P]_t) \times \Delta t \quad \text{……..(Eq. 4)}$$

649 β_m , α_m , β_p and α_p were expressed in appropriate units for further simplification of these equations.
650 The base parameter values for the model were set as: K_{on} = 0.02, K_{off} = 0.2, β_m = 10 per unit time,
651 β_p = 100 per mRNA molecule per unit time, α_m = 0.07 per mRNA molecule per unit time, and α_p
652 = 0.007 per protein molecule per unit time. The dynamics of transcription, variation in the mRNA
653 concentration and variation in protein concentration with time were modeled across 10,000 cells.
654 Noise was expressed as coefficient of variation (CV) from the calculation of mean and standard
655 deviation in the protein level across these 10,000 cells across all time points.
656
657 To investigate how the mean mRNA expression level and the transcriptional burst frequencies
658 combine with translation rate (β_p) and impact protein noise, simulations were performed over a
659 wide range of values of the parameters K_{on} and β_m. The parameter K_{on} was varied between 0.001
660 and 10, and the parameter β_m was varied between 1 to 1000 per unit time. For each value of these
661 parameters, translation rate β_p was varied between a range of 1 to 1000 per mRNA molecule per
662 unit time.
663

664 **Estimation of burst parameters from single-cell RNA-seq data**

665 The two-state model of gene expression enabled estimation of the parameters of transcriptional
666 bursts from single-cell RNA-sequencing data using a maximum likelihood approach, as described
667 by Kim and Marioni [44].

668 Specifically,

669 $$p \mid K_{on}, K_{off} \sim \text{Beta}\ (K_{on}, K_{off}) \quad \ldots\ldots\ldots\ldots\ldots \text{(Eq. 5)}$$

670 $$x \mid \beta_m, p \sim \text{Poisson}\ (\beta_m \cdot p) \quad \ldots\ldots\ldots\ldots\ldots \text{(Eq. 6)}$$

671 where 'x' is the number of RNA transcripts of a given gene within a cell and 'p' is an auxiliary
672 variable following a beta distribution. The mean of the parameter 'p' is equal to the fraction of
673 time that a gene spends in the active state. The resultant marginal distribution is known as Poisson-
674 Beta distribution, denoted by P ($x \mid K_{on}, K_{off}, \beta_m$), and gives the steady-state distribution for the
675 mRNA copy numbers across cells. All parameters are further normalized by α_m. K_{on} and K_{off}
676 control the shape of the Beta distribution and represent the probability of a gene being in 'on' and
677 'off' states, respectively. β_m is the mean of Poisson distribution and represents the average rate of
678 gene expression when the gene is in the 'on' state.

679

680 The yeast single cell RNA-seq data[40] was given as the input to the model. The two-state model
681 parameters $\theta = (K_{on}, K_{off}, \beta_m)$ were inferred by maximizing the likelihood of the parameters of
682 Poisson-Beta distribution for a given set of observed data points X. This can be represented as:

683 $$arg_{max(\theta\ in\ \Theta)} = \prod_{\{x\ in\ X\}} P(x|\theta) \quad \ldots\ldots \text{(Eq. 7)}$$

684

685 This was further represented as maximization of the log-likelihood, which was equivalent to
686 minimization of the negative log-likelihood:

687 $$arg_{max(\theta\ in\ \Theta)} = \sum_{\{x\ in\ X\}} \ln(P(x|\theta)) \quad \ldots\ldots \text{(Eq. 8)}$$

688 $$arg_{min(\theta\ in\ \Theta)} = -\sum_{\{x\ in\ X\}} \ln(P(x|\theta)) \quad \text{..... (Eq. 9)}$$

689

690 The negative log-likelihood was minimized using L-BFGS-B approach[68] and the resulting
691 distributions for parameters in θ were calculated.

692

693 **Mathematical model of translation at single mRNA level for capturing bursty translation**

694 Several mathematical models for the translation process have been described, and they include the
695 TASEP model, the Ribosome Flow Model (RFM) and their variants[45,46,69-72]. Totally Asymmetric
696 Simple Exclusion Process or TASEP model assumes that an mRNA molecule is a one-dimensional
697 lattice through which a ribosome can hop in only one direction from one site to the next, provided
698 the latter is empty.

699

700 To capture the dynamics of translation, a simple TASEP-based model with appropriate
701 modifications was developed and bursty translation was incorporated. To start with, translational
702 bursts were assumed to arise due to stochastic transitions of an mRNA molecule between active
703 and inactive states with the rates TL_{on} and TL_{off} respectively. In the active state, translation
704 initiation on the mRNA molecule occurred at a rate TL_{init}. The parameters TL_{on} and TL_{off} were
705 assumed to follow Poisson distributions individually and hence, the time-intervals between two
706 subsequent on-states (or off-states) were assumed to follow exponential distributions. The
707 parameter values were chosen within the range of parameter values observed or estimated from
708 experimental datasets, to build a realistic model. For yeast genes, maximum likelihood estimates
709 of K_{on} and K_{off} from single-cell RNA-seq data[40] were in the ranges of 0.005 to 744, and 0.001 to
710 1000, respectively. In yeast, the experimental estimates for mRNA synthesis rates ranged from
711 ~0.01 to 4 per min[73], and protein synthesis rates per mRNA ranged from 0-13.6 per sec per mRNA

712 [41]. Earlier Estimates for mRNA half-life ranged from 3 mins to 300 mins[74] but a recent non-
713 invasive measurement of mRNA half-life has found that majority of mRNA molecules in yeast
714 have half-lives of less than 10 mins[64]. The estimates for protein half-life ranged from 2 mins to
715 ~16000 mins[75]. However, no estimates for TL_{on} and TL_{off} were available. Large values of K_{on},
716 TL_{on}, mRNA synthesis rate, protein synthesis rates, mRNA half-life and protein half-life made
717 simulations extremely slow and computationally very demanding, as the model had to track many
718 mRNA molecules and translation initiation events. Therefore, these values were not explored. In
719 addition, genes with very stable mRNA molecules are unlikely to show fluctuation in mRNA
720 numbers and therefore, are not of interest to this study.
721
722 As multiple ribosomes could translate a single mRNA molecule at the same time, a second
723 translation initiation happened only when the earlier mRNA bound ribosome had moved by 10 or
724 more codons on the mRNA molecule, thus, accounting for steric interactions between two
725 ribosomes[47,48]. Movement of ribosome through an mRNA molecule depends on the individual
726 codons that are present. Preferred codons for which tRNA molecules are readily available are
727 traversed quickly, whereas the rare codons are read slower. Tuller *et al.*[34] observed a specific and
728 conserved translational profile across several species where translational efficiency was low at the
729 start of the genes for about 30-50 codons, followed by a gradual increase to the maximum
730 efficiency. Similarly, Weinberg *et al.*[49] observed a slow rate of translation, although to a different
731 degree, in the first 200 nucleotides of a gene. This enabled us to model ribosome traversal speed
732 in a more general manner rather than focusing on the occurrence of specific codons that would
733 vary from one gene to another. The ribosome traversal speed was modeled using a first order Hill
734 function of the following form
735 $V = \frac{V_{max}L}{K_{Hill}+L}$ …… (Eq. 10)

736 Where, V = traversal speed of the ribosome at codon L in the mRNA molecule, V_{max} = maximum
737 traversal speed of the ribosome in the mRNA molecule, K_{Hill} = constant, and L = position in the
738 mRNA. The values of V_{max} and K_{Hill} were chosen to be 100 codons per min and 30 respectively.
739 All parameters were further varied and tested for model robustness as discussed below.
740
741 The value of K_{Hill} influenced the relationship between the traversal speed and the position L, and
742 eventually determined the time taken for a ribosome to completely traverse through a mRNA
743 molecule. High values of K_{Hill} reduced the number of translation initiation events, thus mimicking
744 the scenario of lower translational efficiency. This is because a ribosome took longer time to
745 traverse through the first 10 codons, which was required before the next translation initiation event
746 could take place. A reduction in the value of K_{Hill} allowed higher translation initiation rate (TL_{init})
747 and captured the behavior of the system in case of high translational efficiency. Conversely,
748 increasing the translation initiation rate required the K_{Hill} value to be lower. Thus, the relationship
749 between K_{Hill} and translation initiation rate (TL_{init}) was modeled using the equation
750 $K_{Hill} = A \times (1 + \frac{B}{B+\mathrm{TL}_{init}})$ ….. (Eq. 11)
751 Where A and B were constants. The values of A and B shaped the relationship between K_{Hill} and
752 β_p, and in our model were chosen as 20 and 5 respectively. Higher translational efficiency led to
753 faster traversal of ribosome through an mRNA molecule and allowed more translation initiation
754 events leading to higher value of β_p. The model was tested with different values of the parameters
755 K_{Hill}, A, B and V_{max} to test for robustness.
756
757 In the next step, the model of translation at the single mRNA level was integrated with the two-
758 state model of transcription, and the combined model was utilized for subsequent stochastic
759 simulations. The base parameter values for the model were chosen as: K_{on} = 0.02, K_{off} = 0.2, β_m =

760 4 per minute, TL_{on}=0.5, TL_{off}=0.5, A=20, B=5, K_{Hill}=30, V_{max}=100 codons per minute, Length of
761 the gene (L_{tot}) = 300 codons, mRNA half-life (HL_{mRNA}) = 10 mins, and protein half-life (HL_{prot}) =
762 100 mins.
763
764 Every mRNA molecule generated through transcriptional burst was tracked by the translation
765 model at every minute over the life-time of the mRNA molecule, and the protein expression at
766 every time-point was estimated. Gillespie's algorithm was used for simulations in 1000 cells
767 through which estimates for population-wide mean protein expression and protein noise were
768 derived. The process was repeated for a wide-range of transcriptional and translational burst
769 frequency values, as well as for other parameters of the models, to investigate whether positive
770 correlation between mean protein expression and protein noise could be observed at specific
771 parameter values. The K_{on} parameter was varied between 0.01 and 10, the K_{off} parameter was
772 varied between 0.01 and 10, TL_{on} between 0.01 and 5, TL_{off} between 0.01 and 5, and β_m between
773 0.1 to 20 per min. For each of these parameter values, TL_{init} was varied between 0.1 and 10 per
774 mRNA molecule per minute. The values of mRNA and protein half-lives were stochastically
775 varied by ±10% of the chosen value, as the half-lives of individual mRNA and protein molecules
776 can vary within a cell.
777
778 **Modeling and simulation of demand for ribosomal machinery**
779 As multiple mRNA molecules share a common pool of ribosomal machinery for translation, the
780 number of ribosomes available for translating a specific mRNA molecule can vary with time.
781 Several studies have modeled the translation process with finite resources and competition,
782 however, none of them had investigated the impact on protein expression levels or on
783 heterogeneity. Only one earlier study, investing the stochastic nature of translation using

784 mathematical models, predicted that use of rare codons will increase expression heterogeneity[76],
785 which contradicted the empirical observations.
786
787 Competition for a finite pool of ribosomal machinery would impact the translation initiation rate
788 in an mRNA molecule. High availability of ribosomal machinery would lead to high translation
789 initiation rate, whereas a scarcity of ribosomes would lower translation initiation rate.
790 Transcriptional bursts generate stochastic fluctuations in mRNA numbers over time which can
791 lead to a variable demand for ribosomal machinery required for translation. When the number of
792 mRNA molecules of a gene increases suddenly due to a transcriptional burst, the demand for
793 ribosomal machinery increases rapidly. Subsequently, when the mRNA numbers fall, this lowers
794 demand and frees up ribosomes, which can then be utilized for translating mRNA molecules of
795 other genes.
796
797 The demand for ribosomal machinery was incorporated in the model of translation so that its effect
798 on translation initiation rate of an mRNA molecule could be captured. For a gene, the number of
799 mRNA molecules produced by transcriptional bursting and the number of ribosomes bound to
800 mRNA molecules were tracked over time. At every time point during simulation, the ribosome
801 demand was modeled using different functions that incorporated the ratio of mRNA numbers at
802 the current time point to the mRNA numbers at the previous time point, the ratio of current number
803 of bound ribosomes to the number of bound ribosomes at the previous time point or a combination
804 of both (parameter 'av', Table S1). These included functions where the translation initiation rate
805 at a specific time point was equal to the basal translation initiation rate divided by the ribosome
806 demand, or more complex Hill functions of order 10 (Table S1), that could induce sharp transitions
807 in translation initiation rate when demand was too high. The parameter 'av' modeled the ribosome

808 demand at a specific time point during the simulations, and the parameter 'kc' defined the threshold
809 value for ribosome demand beyond which the translation initiation rate decreased sharply.
810
811 Higher number of mRNA molecules or number of ribosomes bound to mRNA at a time point
812 compared to the previous time point meant lower availability of ribosomal machinery for
813 translation and lower translation initiation rate. Among all functions tested, the one which
814 considered both number of mRNA molecules and number of bound ribosomes at current and
815 previous time points, and modeled the impact of ribosome availability on translation initiation rate
816 through Hill function (Function 14 to Function 19, Table S1) generated the best positive correlation
817 between mean protein expression and protein noise (Fig. S8). The function 16 was used for all
818 subsequent analysis.
819
820 The integrated model of bursty transcription and bursty translation incorporating ribosome demand
821 was tested in a wide range of values of several parameters. The impact of variation in values of
822 the parameters A, B and maximum ribosome traversal rate (V_{max}) individually on correlation
823 between protein noise and translational efficiency was tested. The parameter A was varied between
824 10 and 50, B between 1 and 10, V_{max} between 50 and 150. For each of the parameter values, the
825 translation initiation rate (TL_{init}) was varied between 0.1 and 10 per mRNA molecule per min. For
826 $V_{max} = 50$, no protein expression was observed. For the rest of the parameter values, no effect on
827 correlation between translational efficiency and protein noise was observed (Fig. S9-S11).
828
829 In the next step, the model was tested with different values of the parameters K_{on}, K_{off}, TL_{on}, TL_{off},
830 and β_m. Each of these parameters was varied individually and the impact of changes in the
831 translation initiation rate (TL_{init}) on protein noise was tested (Fig. 4D,E; Fig. S12-S14). The

832 parameter K_{on} was varied between 0.01 and 10, K_{off} between 0.01 and 10, TL_{on} between 0.01 and
833 5, TL_{off} between 0.01 and 5, and β_m between 0.1 and 20. For each of these parameter values, TL_{init}
834 was varied between 0.1 and 10 per mRNA molecule per min. Higher rates of β_m and TL_{init} made
835 simulations extremely slow and computationally very demanding, as the model had to track a large
836 number of mRNA molecules and translation initiation events, respectively. Therefore, these values
837 could not be used for simulation.
838
839 Since it was not possible to explore all possible combinations of parameter values due to an
840 extremely large number of combinations, random sampling of parameter values for K_{on}, K_{off}, TL_{on},
841 TL_{off}, β_m, HL_{mRNA} and $HL_{protein}$ were performed from a specified range of each parameter (Fig.
842 S16). This also enabled us to study how different combinations of values of these parameters
843 impact protein noise, and consequently, the relationship between translational efficiency and
844 protein noise. Fifty random sampling of parameter values were done and for each set of parameter
845 values, the translation rate (β_p) was varied between 0.2 and 10 per mRNA molecule per min. The
846 parameter K_{on} was sampled in the range of 0.01 to 2, K_{off} between 0.01 and 2, TL_{on} between 0.1
847 and 5, β_m between 0.1 and 10 per min, HL_{mRNA} between 1 and 20 mins, and HL_{prot} between 1 and
848 200 mins. Simulation results indicated interactions between different parameter values that also
849 impacted the relationship between translational efficiency and protein noise (Fig. S15).
850
851 **Construction of GFP-promoter fragment and genomic integration in yeast**
852 *Saccharomyces cerevisiae* BY4741 strain was used for experiments. *Green Fluorescent Protein*
853 (*GFP*) gene integrated in the yeast genome was used as the model system for noise quantification.
854 The gene-promoter construct was made as follows. The *GFP* gene was amplified from the yeast
855 strain where the *PDR5* gene was tagged with *GFP,* and the first two codons ATG and TCT were

856 added with the help of primers (Table S2). For PCR amplification, genomic DNA from yeast was
857 isolated by lithium acetate-SDS method and 2 µl genomic DNA was used as template.
858 Amplification using Q5 DNA polymerase and gene-specific primers was performed, and the PCR
859 product subsequently purified using QIA quick PCR Purification Kit (Qiagen).
860
861 The strain BY4741 has a truncated and non-functional *HIS3* gene (*his3Δ1*). Therefore, the gene-
862 promoter construct was inserted into the site of the *HIS3* gene through homologous recombination,
863 and *HIS3MX6* cassette was used as the auxotrophic marker for selection of transformed colonies.
864 The *HIS3MX6* cassette was amplified from yeast strain with *PDR5-GFP* fusion. For genomic
865 integration, the genomic regions upstream and downstream region of the *HIS3* gene, denoted by
866 His3L and His3R respectively (Fig. S17), were amplified and were separately cloned into pUC19
867 vector with restriction digestion and ligation. The constructs were transformed into chemically
868 competent *E. coli* cells[77] and the transformed bacterial colonies were selected on LB plates
869 supplemented with 100 µg/ml ampicillin. The promoters, the *GFP* gene and the *HIS3MX6* cassette
870 were subsequently cloned step-by-step through restriction digestion with appropriate enzymes
871 (Fig. S17), followed by ligation with T4 DNA ligase. The constructs were transformed into *E. coli*
872 and were selected on LB plates supplemented with ampicillin. The cloned DNA fragments were
873 verified by restriction digestion of the constructed fragment, as well as through Sanger sequencing.
874 Promoters of four genes, namely, *RPG1*, *RPL35A*, *CPA2* and *QCR2* were cloned upstream of the
875 *GFP* gene (Table S3). The genes *CPA2* and *QCR2* showed high protein noise and the genes *RPG1*
876 and *RPL35A* showed low protein noise in genome-wide noise data of yeast[15]. For cloning promoter
877 sequence of a gene, the region between the start codon of the gene and the stop codon of the
878 previous gene on the same DNA strand was considered (Table S3).
879

880 In the next step, the full construct was amplified using His3L forward and His3R reverse primers
881 (Table S2) using Q5 polymerase, and 20 µl of the PCR product was used for transformation into
882 competent yeast cells following the protocol of Gietz and Schiestl[78]. Briefly, yeast cells were first
883 grown to saturation in YPD medium at 30°C overnight, and then were diluted into fresh medium,
884 where they were allowed to grow for 4 hours. Cells were precipitated, and were washed once with
885 0.1M lithium acetate (LiAc) solution. Cells were resuspended in 50µl of 0.1M LiAc and then 5µl
886 salmon sperm carrier DNA along with 20µl of PCR product were added. Further, 300 µl of PLI
887 solution, comprising of 10% (v/v) 1M LiAC, 10% (v/v) water and 80% (v/v) PEG 3350 (50%
888 w/v), was added to each tube. Cells were subjected to heat shock at 42°C for 40 minutes, following
889 which PLI solution was removed, and the cells were plated on synthetic complete medium
890 supplemented with 2% glucose but without any histidine (SD-His). Colonies with genomic
891 integration were confirmed by colony PCR, and subsequently, were verified by Sanger sequencing.
892

893 **Generation of single- and multi-mutant variants of GFP**

894 Seven mutant variants of the *GFP* gene were constructed, out of which three variants contained
895 mutations in the N-terminal region and four variants contained mutations in the C-terminal region.
896 Variants with mutations in the N-terminal or C-terminal regions were targeted to prevent
897 disturbing the catalytic core of the GFP protein. The mutant variants were cloned downstream of
898 the four promoters.
899

900 The N-terminal single mutant variants consisted of TCT to TCG (S to S) mutation at codon 2,
901 GGA to GGT (G to G) mutation at codon 4, GAA to GAG (E to E) mutation at codon 5 and GAA
902 to GAC (E to D) mutation at codon 6. The C-terminal single mutants consisted of GAT to GAC
903 (D to D) mutation at codon 234, CTA to CTC (L to L) mutation at codon 236, and AAA to AAG

904 (K to K) mutation at codon 238. The multi-mutant variant at the N-terminal end (denoted by N-5)
905 contained five mutations, namely, TCT to TCG (S to S) at codon 2, AAA to AAG (K to K) at
906 codon 3, GGA to GGT (G to G) at codon 4, GAA to GAG (E to E) at codon 5, and GAA to GAC
907 (E to D) at codon 6. The multi-mutant variant at the C-terminal end (denoted by C-5) contained
908 five mutations, namely, GAT to GAC (D to D) at codon 234, GAA to GAC (E to D) mutation at
909 codon 235, CTA to CTC mutation (L to L) at codon 236, TAC to AAC mutation (Y to N) at codon
910 237, and AAA to AAG mutation (K to K) at codon 238.
911
912 To construct and clone the mutant variants of the GFP gene downstream of the promoter regions,
913 an overlap extension PCR method following the protocol described in Higuchi *et al.*[79] was used.
914 For generating the mutant variants, primers were designed keeping the target mutation at the center
915 with 15 bases flanking them on each side. In the first amplification step, two fragments were
916 generated. The first fragment was from the 5' end of Hi3L region till the targeted mutation site in
917 the *GFP* gene, and the second fragment was from the targeted mutation site in the *GFP* gene till
918 the 3' end region of His3R (Fig. S22). Amplification was carried out using high-fidelity Q5 DNA
919 polymerase. The reaction mixture comprised of 2.5 µl of each primer (10 µM), 10 µl of 5x Q5
920 reaction buffer, 1 µl of 10 mM dNTPs, 0.5 µl of Q5 DNA polymerase (New England Biolabs) and
921 molecular biology grade water to a total volume of 50 µl. The PCR program consisted of
922 incubation at 98 °C for 1 min (initial denaturation) followed by 30 cycles of 98°C for 10 sec
923 (denaturation), 65°C for 30 sec (annealing), 72°C for 1 min 30 sec (extension), and a final
924 extension at 72°C for 10 min.
925
926 The products after amplification were treated with 1 µl of ExoSAP-IT PCR product cleanup
927 reagent (Thermo Fisher Scientific) and 0.5 µl DpnI (New England Biolabs) for 1 hr at 37°C,

928 followed by deactivation for 20 min at 80 °C. The products were then purified using QIAquick
929 PCR Purification Kit (Qiagen) and quantified using Qubit 4 Fluorometer (Thermo Fisher
930 Scientific).
931
932 As the molecular weight of the amplified fragments were variable, equimolar concentration
933 of the fragments from the previous amplification step were used in the next step. For each
934 reaction, 0.5 to 1 picomole of each purified fragment were used as templates. For assembly, the
935 reaction mixture comprised of equimolar content of two template fragments, 10 µl of 5x Q5
936 reaction buffer, 1 µl of 10 mM dNTPs, 0.5 µl of Q5 DNA polymerase (New England Biolabs) and
937 molecular biology grade water to a total volume of 45 µl, without any primer. The program
938 consisted of incubation at 98 °C for 1 min (initial denaturation) followed by 10 cycles of 98°C for
939 10 sec (denaturation), 60°C for 30 sec (annealing) and 72°C for 1 min 30 sec (extension). On
940 completion of 10th cycle, 2.5 µl of forward and reverse primers (10 µM stock of each) were added,
941 and the program was run for next 25 cycles by raising the annealing temperature to 72°C. The
942 reaction was terminated by a final extension at 72°C for 10 min.
943
944 The assembled mutant constructs were then directly transformed into competent yeast cells
945 following the LiAC method as described above, and the transformants were selected on SD-His
946 plates. The clones were confirmed by colony PCR and Sanger sequencing.
947
948 **Measurement of expression noise using flow cytometry**
949 Three clones of wild-type GFP gene and each mutant variant were picked for noise measurement
950 in flow cytometry. Yeast cultures were grown in SCD medium (0.67% YNB + 0.079% complete
951 synthetic supplement + 2% glucose) at 30°C with shaking at 220 rpm. Yeast cells from glycerol

952 stock were inoculated in SCD medium, were grown for 24 hours, and were then diluted 1:100 in
953 fresh medium. This process was repeated one more time. The cells were then diluted 1:50 in fresh
954 SCD and were grown for 4 hours. In the next step, cells were centrifuged and washed twice with
955 1X PBS (Phosphate Buffered Saline) buffer, and were finally resuspended in 1X PBS buffer for
956 flow cytometry. In flow cytometry, the data were acquired for 2,00,000 cells for each sample in a
957 BD LSR Fortessa cell analyzer (Fig. S18). To minimize heterogeneity in signal due to
958 heterogeneity in cell size and complexity, a small homogeneous subset of cells with similar size
959 and complexity parameters (FSC-A and SSC-A) were filtered. Ellipses with different lengths of
960 major and minor axes were fitted to the FSC-A vs SSC-A plot, and the best fit that covered the
961 most of homogeneous cells was chosen (Fig. S19). This also filtered out cell aggregates or budding
962 cells which can have higher GFP signal than single cells. The data from these cells were then used
963 for calculation of expression noise. The data were analyzed using custom R codes based on codes
964 from Silander *et al.*[14]. Normalized mean expression and normalized noise value for a strain in an
965 experiment was calculated by dividing the mean expression and noise values with the
966 corresponding values for the wild-type variant in that experiment.
967

968
969

References

1. N. Q. Balaban, J. Merrin, R. Chait, L. Kowalik, S. Leibler, Bacterial persistence as a phenotypic switch. *Science* **305**, 1622-1625 (2004). doi: 10.1126/science.1099390.

2. Y. Wakamoto, N. Dhar, R. Chait, K. Schneider, F. Signorino-Gelo, S. Leibler, J. D. McKinney, Dynamic persistence of antibiotic-stressed mycobacteria. *Science* **339**, 91-95 (2013). doi: 10.1126/science.1229858.

3. A. Raj, S. A. Rifkin, E. Andersen, A. van Oudenaarden, Variability in gene expression underlies incomplete penetrance. *Nature* **463**, 913-918 (2010). doi: 10.1038/nature08781.

4. A. Burga, M. O. Casanueva, B. Lehner, Predicting mutation outcome from early stochastic variation in genetic interaction partners. *Nature* **480**, 250-253 (2011). doi: 10.1038/nature10665.

5. A. Eldar, V. K. Chary, P. Xenopoulos, M. E. Fontes, O. C. Losón, J. Dworkin, P. J. Piggot, M. B. Elowitz, Partial penetrance facilitates developmental evolution in bacteria. *Nature* **460**, 510-514 (2009). doi: 10.1038/nature08150.

6. Y. Lu, K. Bohn-Wippert, P. J. Pazerunas, J. M. Moy, H. Singh, R. D. Dar, Screening for gene expression fluctuations reveals latency-promoting agents of HIV. *Proc Natl Acad Sci USA* **118**, e2012191118 (2021). doi: 10.1073/pnas.2012191118.

7. M. A. Coomer, L. Ham, M. P. H. Stumpf, Noise distorts the epigenetic landscape and shapes cell-fate decisions. *Cell Syst.* **13**, 83-102.e6 (2022). doi: 10.1016/j.cels.2021.09.002.

8. A. Nguyen, M. Yoshida, H. Goodarzi, S. F. Tavazoie, Highly variable cancer subpopulations that exhibit enhanced transcriptome variability and metastatic fitness. *Nat Commun*. **7**, 11246 (2016). doi: 10.1038/ncomms11246.

9. A. Sharma, E. Merritt, X. Hu, A. Cruz, C. Jiang, H. Sarkodie, Z. Zhou, J. Malhotra, G. M. Riedlinger, S. De, Non-Genetic Intra-Tumor Heterogeneity Is a Major Predictor of Phenotypic Heterogeneity and Ongoing Evolutionary Dynamics in Lung Tumors. *Cell Rep*. **29**, 2164-2174.e5 (2019). doi: 10.1016/j.celrep.2019.10.045.

10. B. L. Emert, C. J. Cote, E. A. Torre, I. P. Dardani, C. L. Jiang, N. Jain, S. M. Shaffer, A. Raj, Variability within rare cell states enables multiple paths toward drug resistance. *Nat Biotechnol*. **39**, 865-876 (2021). doi: 10.1038/s41587-021-00837-3.

11. I. Golding, J. Paulsson, S. M. Zawilski, E. C. Cox, Real-time kinetics of gene activity in individual bacteria. *Cell* **123**,1025-1036 (2005). doi: 10.1016/j.cell.2005.09.031.

12. L. Cai, N. Friedman, X. S. Xie, Stochastic protein expression in individual cells at the single molecule level. *Nature* **440**, 358-62 (2006). doi: 10.1038/nature04599.

13. A. Raj, C. S. Peskin, D. Tranchina, D. Y. Vargas, S. Tyagi, Stochastic mRNA synthesis in mammalian cells. *PLoS Biol.* **4**, e309 (2006). doi: 10.1371/journal.pbio.0040309.

14. O. K. Silander, N. Nikolic, A. Zaslaver, A. Bren, I. Kikoin, U. Alon, M. Ackermann, A genome-wide analysis of promoter-mediated phenotypic noise in *Escherichia coli*. *PLoS Genet.* **8**, e1002443 (2012). doi: 10.1371/journal.pgen.1002443.

15. J. R. Newman, S. Ghaemmaghami, J. Ihmels, D. K. Breslow, M. Noble, J. L. DeRisi, J. S. Weissman, Single-cell proteomic analysis of *S. cerevisiae* reveals the architecture of biological noise. *Nature*, **441,** 840-846 (2006). doi: 10.1038/nature04785.

16. A. Bar-Even, J. Paulsson, N. Maheshri, M. Carmi, E. O'Shea, Y. Pilpel, N. Barkai, Noise in protein expression scales with natural protein abundance. *Nat Genet.* **38,** 636-643 (2006). doi: 10.1038/ng1807.

17. D. M. Suter, N. Molina, D. Gatfield, K. Schneider, U. Schibler, F. Naef, Mammalian genes are transcribed with widely different bursting kinetics. *Science* **332**, 472-4 (2011). doi: 10.1126/science.1198817.

18. R. D. Dar, B. S. Razooky, A. Singh, T. V. Trimeloni, J. M. McCollum, C. D. Cox, M. L. Simpson, L. S. Weinberger, Transcriptional burst frequency and burst size are equally modulated across the human genome. *Proc Natl Acad Sci USA* **109**, 17454-17459 (2012). doi: 10.1073/pnas.1213530109

19. I. Tirosh, A. Weinberger, M. Carmi, N. Barkai, A genetic signature of interspecies variations in gene expression. *Nat Genet.* **38**, 830-834 (2006). doi: 10.1038/ng1819.

20. J. M. Raser, E. K. O'Shea, Control of stochasticity in eukaryotic gene expression. *Science* **304**, 1811-1814 (2004). doi: 10.1126/science.1098641.

21. C. N. Ravarani, G. Chalancon, M. Breker, N. S. de Groot, M. M. Babu, Affinity and competition for TBP are molecular determinants of gene expression noise. *Nat Commun*. **7,** 10417 (2016). doi: 10.1038/ncomms10417.

22. I. Tirosh, N. Barkai, Two strategies for gene regulation by promoter nucleosomes. *Genome Res.* **18**, 1084-1091 (2008). doi: 10.1101/gr.076059.108.

23. J. K. Choi, Y. J. Kim, Intrinsic variability of gene expression encoded in nucleosome positioning sequences. *Nat Genet*. **41**, 498-503 (2009). doi: 10.1038/ng.319.

24. X. Chen, J. Zhang, The Genomic Landscape of Position Effects on Protein Expression Level and Noise in Yeast. *Cell Syst.* **2**, 347-354 (2016). doi: 10.1016/j.cels.2016.03.009.

25. A. J. Faure, J. M. Schmiedel, B. Lehner, Systematic Analysis of the Determinants of Gene Expression Noise in Embryonic Stem Cells. *Cell Syst.* **5**, 471-484.e4 (2017). doi: 10.1016/j.cels.2017.10.003.

26. B. T. Donovan, A. Huynh, D. A. Ball, H. P. Patel, M. G. Poirier, D. R. Larson, M. L. Ferguson, T. L. Lenstra. Live-cell imaging reveals the interplay between transcription factors, nucleosomes, and bursting. *EMBO J*. **38**, e100809 (2019). doi: 10.15252/embj.2018100809.

1065
1066 27. K. Loell, Y. Wu, M. V. Staller, B. Cohen, Activation domains can decouple the mean and
1067 noise of gene expression. *Cell Rep.* **40**, 111118 (2022). doi: 10.1016/j.celrep.2022.111118.
1068
1069 28. L. Parab, S. Pal, R. Dhar, Transcription factor binding process is the primary driver of noise
1070 in gene expression. *PLoS Genet.* **18**, e1010535 (2022). doi: 10.1371/journal.pgen.1010535.
1071
1072 29. Y. Taniguchi, P. J. Choi, G. W. Li, H. Chen, M. Babu, J. Hearn, A. Emili, X. S. Xie,
1073 Quantifying *E. coli* proteome and transcriptome with single-molecule sensitivity in single cells.
1074 *Science* **329**, 533-538 (2010). doi: 10.1126/science.1188308.
1075
1076 30. E. M. Ozbudak, M. Thattai, I. Kurtser, A. D. Grossman, A. van Oudenaarden, Regulation of
1077 noise in the expression of a single gene. *Nat Genet.* **31**, 69-73 (2002). doi: 10.1038/ng869.
1078
1079 31. W. J. Blake, M. Kaern, C. R. Cantor, J. J. Collins, Noise in eukaryotic gene expression.
1080 *Nature* 422, 633-637 (2003). doi: 10.1038/nature01546.
1081
1082 32. R. Salari, D. Wojtowicz, J. Zheng, D. Levens, Y. Pilpel, T. M. Przytycka, Teasing apart
1083 translational and transcriptional components of stochastic variations in eukaryotic gene
1084 expression. *PLoS Comput Biol.* **8**, e1002644 (2012). doi: 10.1371/journal.pcbi.1002644.
1085
1086 33 M. dos Reis, R. Savva, L. Wernisch, Solving the riddle of codon usage preferences: a test for
1087 translational selection. *Nucleic Acids Res.* 32, 5036-44 (2004). doi: 10.1093/nar/gkh834.
1088
1089 34. T. Tuller, A. Carmi, K. Vestsigian, S. Navon, Y. Dorfan, J. Zaborske, T. Pan, O. Dahan, I.
1090 Furman, Y. Pilpel, An evolutionarily conserved mechanism for controlling the efficiency of
1091 protein translation. *Cell* **141,** 344-354 (2010). doi: 10.1016/j.cell.2010.03.031.
1092
1093 35. H. W. Wu, E. Fajiculay, J. F. Wu, C. S. Yan, C. P. Hsu, S. H. Wu, Noise reduction by
1094 upstream open reading frames. *Nat Plants*. **8,** 474-480 (2022). doi: 10.1038/s41477-022-01136-
1095 8.
1096
1097 36. H. B. Fraser, A. E. Hirsh, G. Giaever, J. Kumm, M. B. Eisen, Noise minimization in
1098 eukaryotic gene expression. *PLoS Biol*. **2**, e137 (2004). doi: 10.1371/journal.pbio.0020137.
1099
1100 37. Y. Pilpel, "Noise in biological systems: pros, cons, and mechanisms of control" in *Yeast*
1101 *Systems Biology* (Humana Press, 2011) pp. 407-25. doi: 10.1007/978-1-61779-173-4_23.
1102
1103 38. B. Wu, C. Eliscovich, Y. J. Yoon, R. H. Singer, Translation dynamics of single mRNAs in
1104 live cells and neurons. *Science* **352**, 1430-1435 (2016). doi: 10.1126/science.aaf1084.
1105
1106 39. N. M. Livingston, J. Kwon, O. Valera, J. A. Saba, N. K. Sinha, P. Reddy, B. Nelson, C.
1107 Wolfe, T. Ha, R. Green, J. Liu, B. Wu, Bursting translation on single mRNAs in live cells. *Mol*
1108 *Cell.* **83**, 2276-2289.e11 (2023). doi: 10.1016/j.molcel.2023.05.019.
1109
1110 40. M. Nadal-Ribelles, S. Islam, W. Wei, P. Latorre, M. Nguyen, E. de Nadal, F. Posas, L. M.
1111 Steinmetz, Sensitive high-throughput single-cell RNA-seq reveals within-clonal transcript

correlations in yeast populations. *Nat Microbiol*. **4**, 683-692 (2019). doi: 10.1038/s41564-018-0346-9.

41. A. Riba, N. Di Nanni, N. Mittal, E. Arhné, A. Schmidt, M. Zavolan, Protein synthesis rates and ribosome occupancies reveal determinants of translation elongation rates. *Proc Natl Acad Sci USA* **116**:15023-15032 (2019). doi: 10.1073/pnas.1817299116.

42. J. Peccoud, B. Ycart, Markovian modeling of gene-product synthesis. *Theor. Popul. Biol*. **48**, 222-234 (1995).

43. D. T. Gillespie, Exact stochastic simulation of coupled chemical reactions. *J. Phys*. *Chem*. **81**, 2340–2361 (1977).

44. J. K. Kim, J. C. Marioni, Inferring the kinetics of stochastic gene expression from single-cell RNA-sequencing data. *Genome Biol.* **14**, R7 (2013). doi: 10.1186/gb-2013-14-1-r7.

45. R.K.P. Zia, J. J. Dong, B. Schmittmann, Modeling Translation in Protein Synthesis with TASEP: A Tutorial and Recent Developments. *J Stat Phys* **144**, 405–428 (2011).

46. D. E. Andreev, M. Arnold, S. J. Kiniry, G. Loughran, A. M. Michel, D. Rachinskii, P. V. Baranov, TASEP modelling provides a parsimonious explanation for the ability of a single uORF to derepress translation during the integrated stress response. *Elife* **7,** e32563 (2018). doi: 10.7554/eLife.32563.

47. J. A. Steitz, Polypeptide chain initiation: nucleotide sequences of the three ribosomal binding sites in bacteriophage R17 RNA. *Nature* **224,** 957-964 (1969). doi: 10.1038/224957a0.

48. N. T. Ingolia, S. Ghaemmaghami, J. R. Newman, J. S. Weissman, Genome-wide analysis in vivo of translation with nucleotide resolution using ribosome profiling. *Science* **324**, 218-223 (2009). doi: 10.1126/science.1168978.

49. D. E. Weinberg, P. Shah, S. W. Eichhorn, J. A. Hussmann, J. B. Plotkin, D. P. Bartel. Improved Ribosome-Footprint and mRNA Measurements Provide Insights into Dynamics and Regulation of Yeast Translation. *Cell Rep*. **14**, 1787-1799 (2016). doi: 10.1016/j.celrep.2016.01.043.

50. C. L. Barrington, G. Galindo, A. L. Koch, E. R. Horton, E. J. Morrison, S. Tisa, T. J. Stasevich, O. S. Rissland. Synonymous codon usage regulates translation initiation. *Cell Rep.* **42**, 113413 (2023). doi: 10.1016/j.celrep.2023.113413.

51. D. Chu, D. J. Barnes, T. von der Haar, The role of tRNA and ribosome competition in coupling the expression of different mRNAs in *Saccharomyces cerevisiae*. *Nucleic Acids Res*. **39,** 6705-14 (2011). doi: 10.1093/nar/gkr300.

52. P. M. Caveney, S. E. Norred, C. W. Chin, J. B. Boreyko, B. S. Razooky, S. T. Retterer, C. P. Collier, M. L. Simpson, Resource Sharing Controls Gene Expression Bursting. *ACS Synth Biol*. **6**, 334-343 (2017). doi: 10.1021/acssynbio.6b00189.

1160
1161 53. Y. Liu, A code within the genetic code: codon usage regulates co-translational protein
1162 folding. *Cell Commun Signal*. **18**, 145 (2020). doi: 10.1186/s12964-020-00642-6.
1163
1164 54. P. S. Spencer, E. Siller, J. F. Anderson, J. M. Barral, Silent substitutions predictably alter
1165 translation elongation rates and protein folding efficiencies. *J Mol Biol*. **422**, 328-335 (2012).
1166 doi: 10.1016/j.jmb.2012.06.010.
1167
1168 55. E. P. O'Brien, M. Vendruscolo, C. M. Dobson, Kinetic modelling indicates that fast-
1169 translating codons can coordinate cotranslational protein folding by avoiding misfolded
1170 intermediates. *Nat Commun.***5**, 2988 (2014). doi: 10.1038/ncomms3988.
1171
1172 56. F. Trovato, E. P. O'Brien, Fast Protein Translation Can Promote Co- and Posttranslational
1173 Folding of Misfolding-Prone Proteins. *Biophys J*. **112**, 1807-1819 (2017). doi:
1174 10.1016/j.bpj.2017.04.006.
1175
1176 57. C. L. Simms, L. L. Yan, H. S. Zaher, Ribosome Collision Is Critical for Quality Control
1177 during No-Go Decay. *Mol Cell*. **68**, 361-373.e5 (2017). doi: 10.1016/j.molcel.2017.08.019.
1178
1179 58. S. Juszkiewicz, G. Slodkowicz, Z. Lin, P. Freire-Pritchett, S. Y. Peak-Chew, R. S. Hegde,
1180 Ribosome collisions trigger cis-acting feedback inhibition of translation initiation. *Elife* **9**,
1181 e60038 (2020). doi: 10.7554/eLife.60038.
1182
1183 59. K. Saito, H. Kratzat, A. Campbell, R. Buschauer, A. M. Burroughs, O. Berninghausen, L.
1184 Aravind, R. Green, R. Beckmann, A. R. Buskirk, Ribosome collisions induce mRNA cleavage
1185 and ribosome rescue in bacteria. *Nature* **603**, 503-508 (2022). doi: 10.1038/s41586-022-04416-7.
1186
1187 60. E. Mordret, O. Dahan, O. Asraf, R. Rak, A. Yehonadav, G. D. Barnabas, J. Cox, T. Geiger,
1188 A. B. Lindner, Y. Pilpel, Systematic Detection of Amino Acid Substitutions in Proteomes
1189 Reveals Mechanistic Basis of Ribosome Errors and Selection for Translation Fidelity. *Mol Cell*.
1190 **75**, 427-441.e5 (2019). doi: 10.1016/j.molcel.2019.06.041.
1191
1192 61. M. Sun, J. Zhang, Preferred synonymous codons are translated more accurately: Proteomic
1193 evidence, among-species variation, and mechanistic basis. *Sci Adv*. **8,** eabl9812 (2022). doi:
1194 10.1126/sciadv.abl9812.
1195
1196 62. P. Dave, G. Roth, E. Griesbach, D. Mateju, T. Hochstoeger, J. A. Chao. Single-molecule
1197 imaging reveals translation-dependent destabilization of mRNAs. *Mol Cell.* **83**, 589-606.e6
1198 (2023). doi: 10.1016/j.molcel.2023.01.013.
1199
1200 63. V. Presnyak, N. Alhusaini, Y. H. Chen, S. Martin, N. Morris, N. Kline, S. Olson, D.
1201 Weinberg, K. E. Baker, B. R. Graveley, J. Coller. Codon optimality is a major determinant of
1202 mRNA stability. *Cell* **160**, 1111-24 (2015). doi: 10.1016/j.cell.2015.02.029.
1203
1204
1205 64. L. Y. Chan, C. F. Mugler, S. Heinrich, P. Vallotton, K. Weis. Non-invasive measurement of
1206 mRNA decay reveals translation initiation as the major determinant of mRNA stability. *Elife* **7**,
1207 e32536 (2018). doi: 10.7554/eLife.32536.

65. K. Leppek, R. Das, M. Barna, Functional 5' UTR mRNA structures in eukaryotic translation regulation and how to find them. *Nat Rev Mol Cell Biol*. **19**, 158-174 (2018). doi: 10.1038/nrm.2017.103.

66. C. A. Charneski, L. D. Hurst, Positively charged residues are the major determinants of ribosomal velocity. *PLoS Biol.* **11**, e1001508 (2013). doi: 10.1371/journal.pbio.1001508.

67. R. Sabi, T. Tuller, Modelling the efficiency of codon-tRNA interactions based on codon usage bias. *DNA Res.* **21**, 511-526 (2014). doi: 10.1093/dnares/dsu017.

68. D. C. Liu, J. Nocedal, On the limited memory BFGS method for large scale optimization. *Mathematical Programming* **45**, 503–528 (1989).

69. S. Reuveni, I. Meilijson, M. Kupiec, E. Ruppin, T. Tuller, Genome-scale analysis of translation elongation with a ribosome flow model. *PLoS Comput Biol.* **7**, e1002127 (2011). doi: 10.1371/journal.pcbi.1002127.

70. L. J. Cook, R. K. Zia, B. Schmittmann, Competition between multiple totally asymmetric simple exclusion processes for a finite pool of resources. *Phys Rev E Stat Nonlin Soft Matter Phys*. **80**, 031142 (2009). doi: 10.1103/PhysRevE.80.031142.

71. C. A. Brackley, M. C. Romano, M. Thiel, The dynamics of supply and demand in mRNA translation. *PLoS Comput Biol.* **7**, e1002203 (2011). doi: 10.1371/journal.pcbi.1002203.

72. A. Jain, M. Margaliot, A. K. Gupta, Large-scale mRNA translation and the intricate effects of competition for the finite pool of ribosomes. *J R Soc Interface* **19,** 20220033 (2022). doi: 10.1098/rsif.2022.0033.

73. C. Miller, B. Schwalb, K. Maier, D. Schulz, S. Dümcke, B. Zacher, A. Mayer, J. Sydow, L. Marcinowski, L. Dölken, D. E. Martin, A. Tresch, P. Cramer, Dynamic transcriptome analysis measures rates of mRNA synthesis and decay in yeast. *Mol Syst Biol*. **7,** 458 (2011). doi: 10.1038/msb.2010.112.

74. J. V. Geisberg, Z. Moqtaderi, X. Fan, F. Ozsolak, K. Struhl, Global analysis of mRNA isoform half-lives reveals stabilizing and destabilizing elements in yeast. *Cell* **156**, 812-824 (2014). doi: 10.1016/j.cell.2013.12.026.

75. A. Belle, A. Tanay, L. Bitincka, R. Shamir, E. K. O'Shea, Quantification of protein half-lives in the budding yeast proteome. *Proc Natl Acad Sci USA* **103**, 13004-13009 (2006). doi: 10.1073/pnas.0605420103.

76. A. Garai, D. Chowdhury, T. V. Ramakrishnan, Fluctuations in protein synthesis from a single RNA template: stochastic kinetics of ribosomes. *Phys Rev E Stat Nonlin Soft Matter Phys*. **79**, 011916 (2009). doi: 10.1103/PhysRevE.79.011916.

1256 77. A. Nishimura, M. Morita, Y. Nishimura, Y Sugino, A rapid and highly efficient method for
1257 preparation of competent Escherichia coli cells. *Nucleic Acids Res*. **18**, 6169 (1990). doi:
1258 10.1093/nar/18.20.6169.
1259
1260 78. R. D. Gietz, R. H. Schiestl, High-efficiency yeast transformation using the LiAc/SS carrier
1261 DNA/PEG method. *Nat Protoc*. **2**, 31-34 (2007). doi: 10.1038/nprot.2007.13.
1262
1263 79. R. Higuchi, B. Krummel, R. K. Saiki, A general method of in vitro preparation and specific
1264 mutagenesis of DNA fragments: study of protein and DNA interactions. *Nucleic Acids Res.* **16**,
1265 7351-7367 (1988). doi: 10.1093/nar/16.15.7351.
1266
1267
1268
1269
1270
1271
1272
1273
1274
1275
1276
1277

Acknowledgments

The authors are thankful to the members of the lab of Dr. Gayatri Mukherjee, School of Medical Science and Technology, IIT Kharagpur for help with flow cytometry.

Financial disclosure statement

This work was supported by funding from IIT Kharagpur ISIRD grant and Science and Engineering Research Board (SERB) grant ECR/2017/002328 to RD. The funders had no role in study design, data collection and analysis, decision to publish or preparation of the manuscript.

Author contributions

Conceptualization: RD

Methodology: SP, UR, RD

Investigation: SP, UR, RD

Visualization: SP, UR, RD

Funding acquisition: RD

Project administration: RD

Supervision: RD

Writing – original draft: SP, UR, RD

Writing – review & editing: SP, UR, RD

Competing interests

The authors have declared that no competing interests exist.

Data availability

Flow cytometry data are available in github:

https://github.com/riddhimandhar/TranslationModNoise

and dryad: https://doi.org/10.5061/dryad.tb2rbp06x

https://datadryad.org/stash/share/D8AhKWZIiouA5HNG9fjUytzetVlz_AOCagXsKcID0WI

Code availability

All codes for data analysis and models are available in github:
https://github.com/riddhimandhar/TranslationModNoise

Supplementary Materials

Figs. S1 to S21

Tables S1 to S3

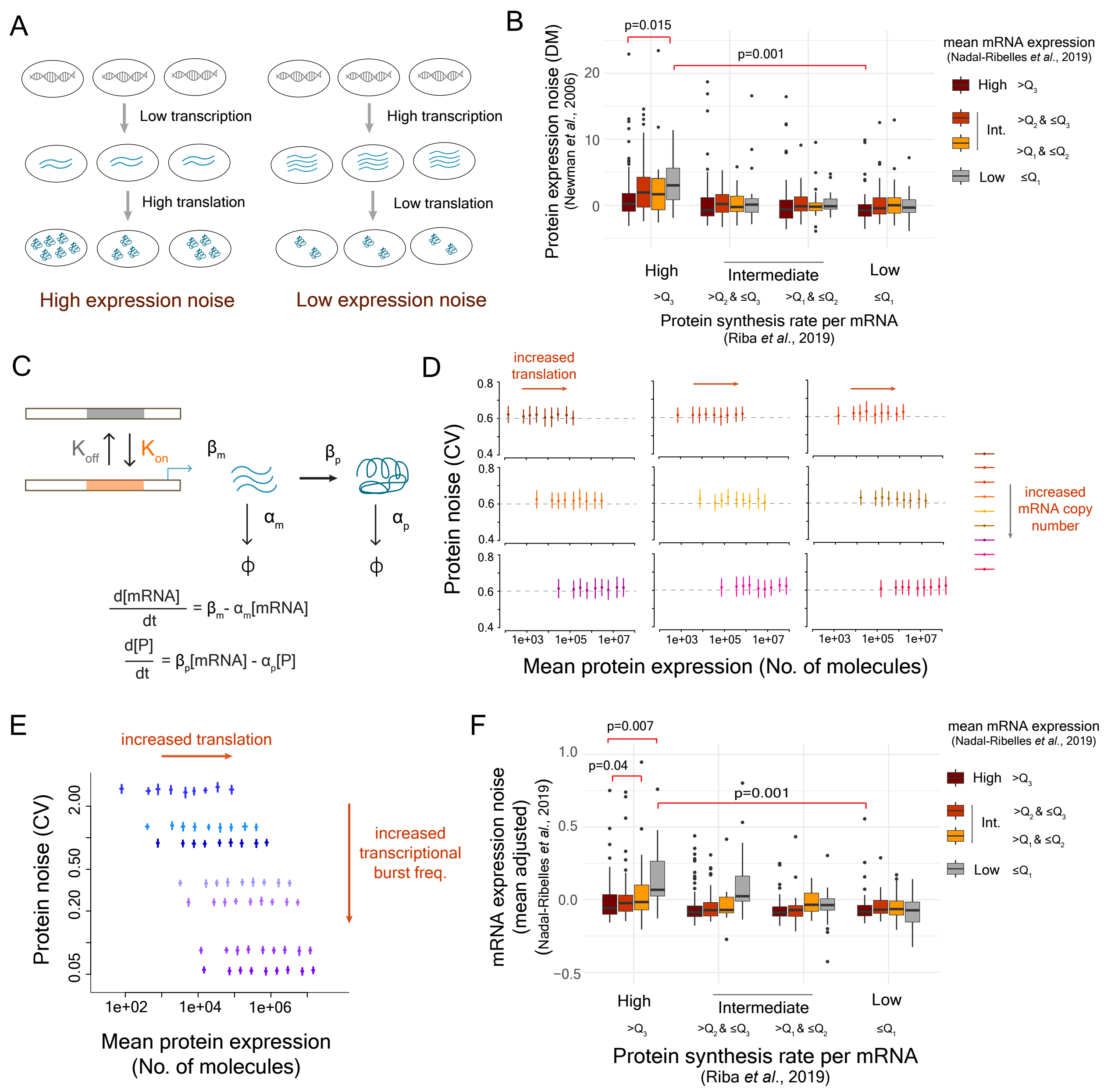
A
Low transcription
High translation
High expression noise
High transcription
Low translation
Low expression noise
B
p=0.015
p=0.001
Protein expression noise (DM)
(Newman et al., 2006)
mean mRNA expression
(Nadal-Ribelles et al., 2019)
High >Q3
Int. >Q2 & ≤Q3
>Q1 & ≤Q2
Low ≤Q1
High
Intermediate
Low
Protein synthesis rate per mRNA
(Riba et al., 2019)
C
Koff
Kon
βm
βp
αm
αp
d[mRNA]/dt = βm - αm[mRNA]
d[P]/dt = βp[mRNA] - αp[P]
D
increased translation
Protein noise (CV)
increased mRNA copy number
Mean protein expression (No. of molecules)
E
increased translation
Protein noise (CV)
increased transcriptional burst freq.
Mean protein expression
(No. of molecules)
F
p=0.007
p=0.04
p=0.001
mRNA expression noise
(mean adjusted)
(Nadal-Ribelles et al., 2019)
mean mRNA expression
(Nadal-Ribelles et al., 2019)
High >Q3
Int. >Q2 & ≤Q3
>Q1 & ≤Q2
Low ≤Q1
High
Intermediate
Low
Protein synthesis rate per mRNA
(Riba et al., 2019)

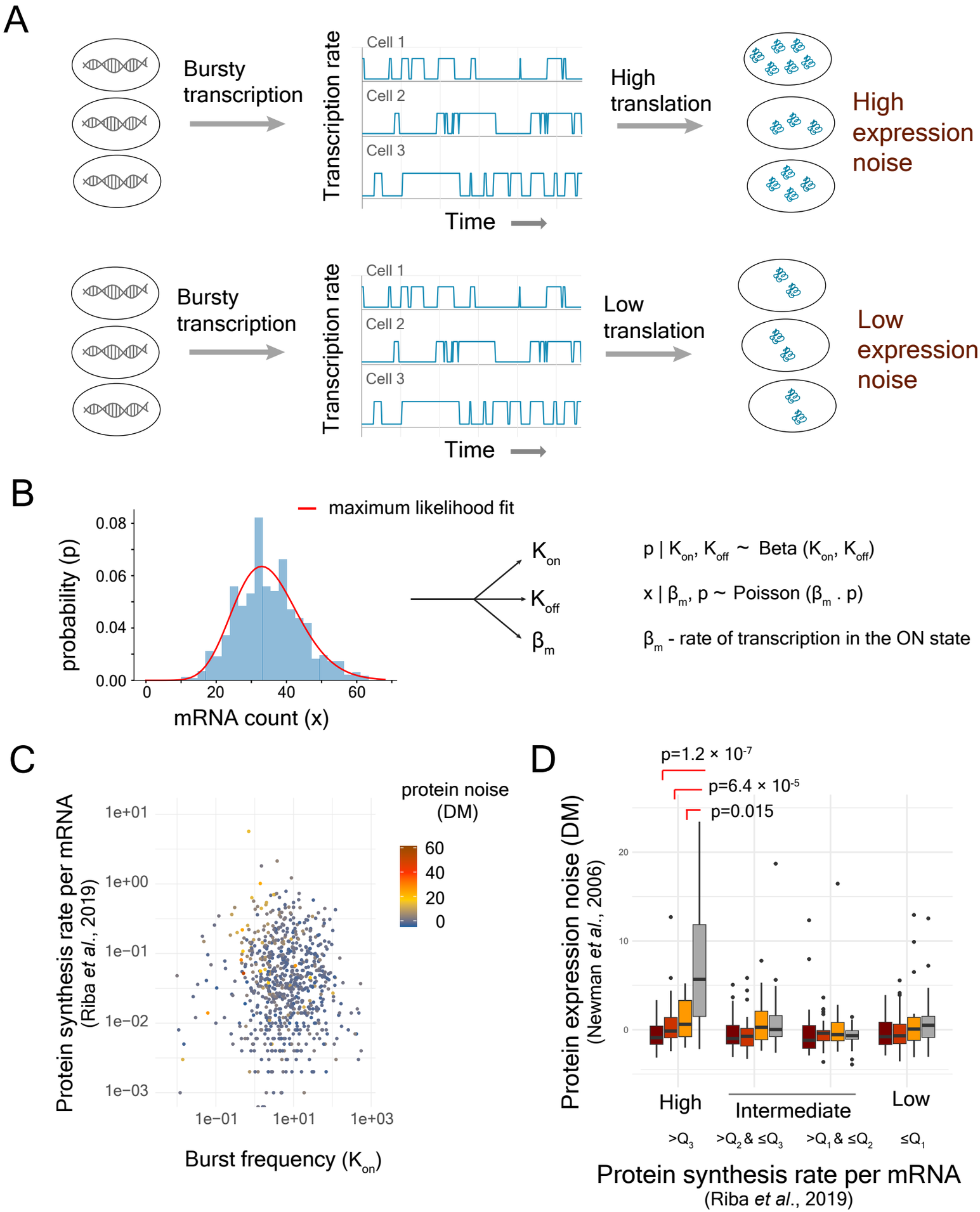
A
Bursty transcription
Transcription rate
Cell 1
Cell 2
Cell 3
Time
High translation
High expression noise
Bursty transcription
Transcription rate
Cell 1
Cell 2
Cell 3
Time
Low translation
Low expression noise
B
maximum likelihood fit
probability (p)
0.08
0.06
0.04
0.00
0
20
40
60
mRNA count (x)
K_{on}
K_{off}
β_m
$p \mid K_{on}, K_{off} \sim \text{Beta}(K_{on}, K_{off})$
$x \mid \beta_m, p \sim \text{Poisson}(\beta_m \cdot p)$
β_m - rate of transcription in the ON state
C
Protein synthesis rate per mRNA
(Riba et al., 2019)
1e+01
1e+00
1e−01
1e−02
1e−03
1e−01
1e+01
1e+03
Burst frequency (K_{on})
protein noise
(DM)
60
40
20
0
D
p=1.2 × 10^{-7}
p=6.4 × 10^{-5}
p=0.015
Protein expression noise (DM)
(Newman et al., 2006)
20
10
0
High
Intermediate
Low
$>Q_3$
$>Q_2$ & $\leq Q_3$
$>Q_1$ & $\leq Q_2$
$\leq Q_1$
Protein synthesis rate per mRNA
(Riba et al., 2019)
Burst freq.
(K_{on})
High $>Q_3$
Int.
$>Q_2$ & $\leq Q_3$
$>Q_1$ & $\leq Q_2$
Low $\leq Q_1$

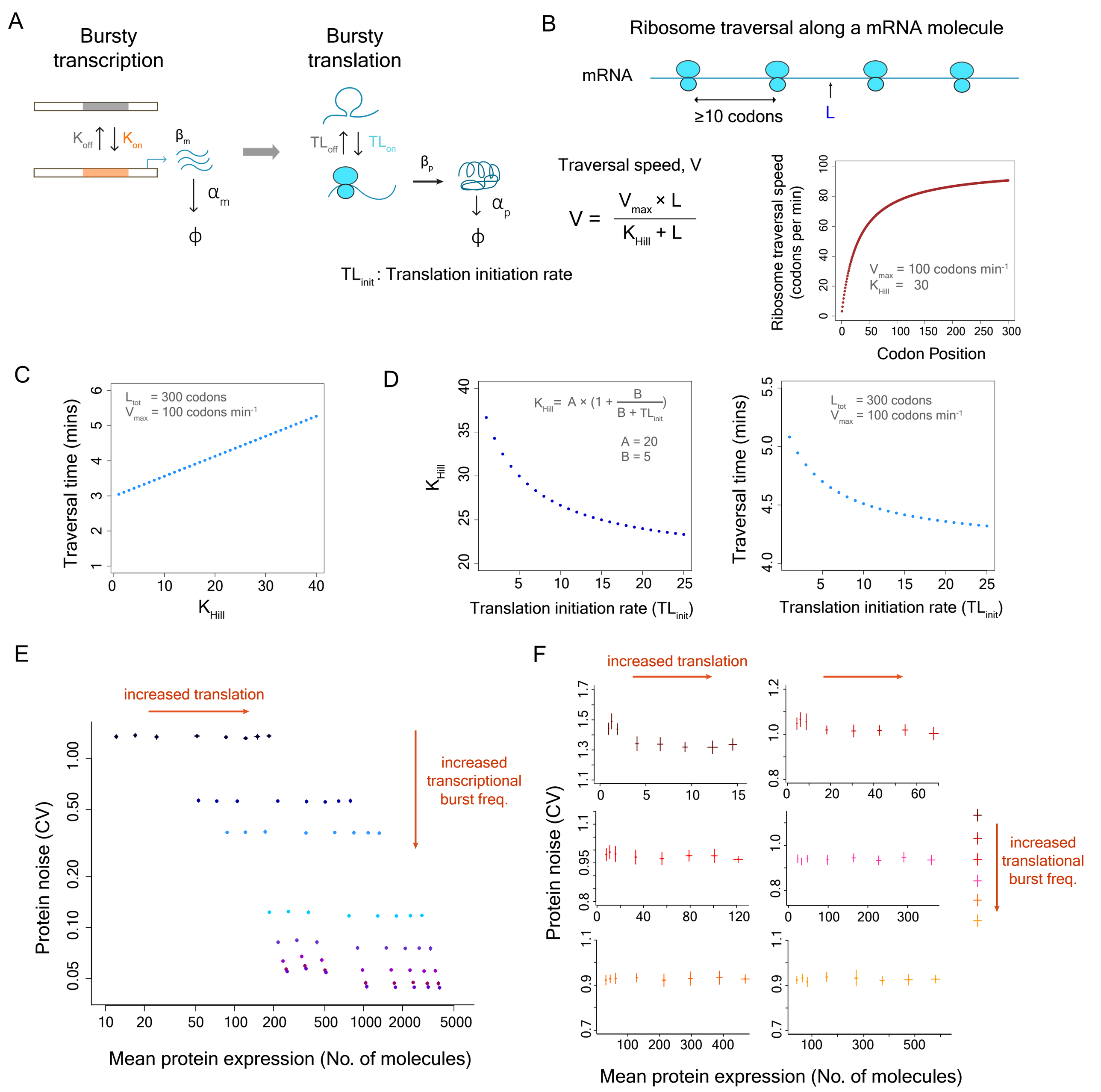
A
Bursty transcription
Bursty translation
K_{off}
K_{on}
β_m
α_m
ϕ
TL_{off}
TL_{on}
β_p
α_p
ϕ
TL_{init} : Translation initiation rate
B
Ribosome traversal along a mRNA molecule
mRNA
≥10 codons
L
Traversal speed, V
$V = \frac{V_{max} \times L}{K_{Hill} + L}$
Ribosome traversal speed (codons per min)
V_{max} = 100 codons min^{-1}
K_{Hill} = 30
Codon Position
C
Traversal time (mins)
L_{tot} = 300 codons
V_{max} = 100 codons min^{-1}
K_{Hill}
D
$K_{Hill} = A \times (1 + \frac{B}{B + TL_{init}})$
A = 20
B = 5
K_{Hill}
Translation initiation rate (TL_{init})
Traversal time (mins)
L_{tot} = 300 codons
V_{max} = 100 codons min^{-1}
Translation initiation rate (TL_{init})
E
increased translation
increased transcriptional burst freq.
Protein noise (CV)
Mean protein expression (No. of molecules)
F
increased translation
increased translational burst freq.
Protein noise (CV)
Mean protein expression (No. of molecules)

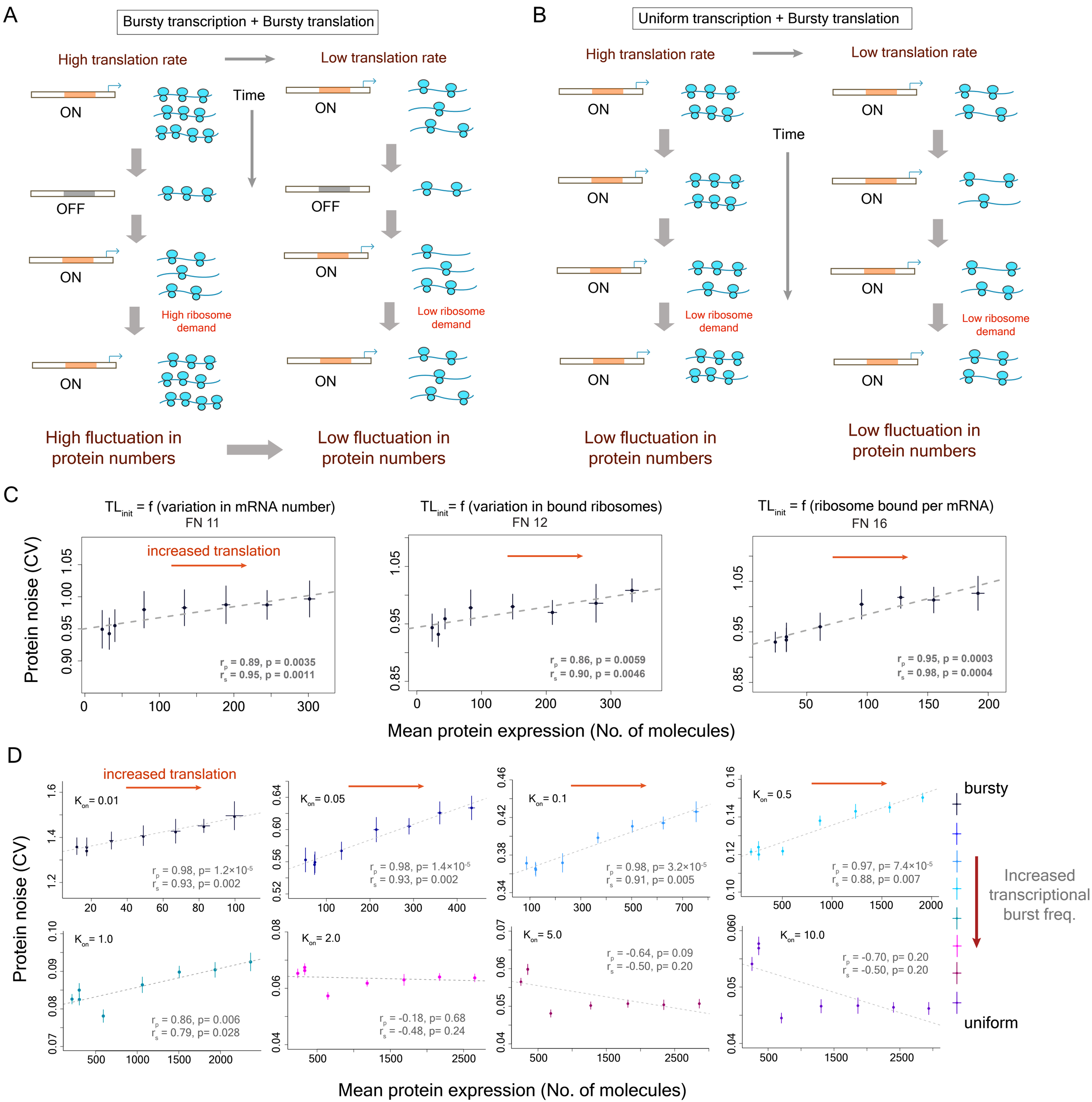
A
Bursty transcription + Bursty translation
High translation rate
Low translation rate
Time
ON
OFF
ON
High ribosome demand
Low ribosome demand
High fluctuation in protein numbers
Low fluctuation in protein numbers
B
Uniform transcription + Bursty translation
High translation rate
Low translation rate
Time
ON
Low ribosome demand
Low fluctuation in protein numbers
Low fluctuation in protein numbers
C
TL_init = f (variation in mRNA number)
FN 11
TL_init = f (variation in bound ribosomes)
FN 12
TL_init = f (ribosome bound per mRNA)
FN 16
increased translation
Protein noise (CV)
r_p = 0.89, p = 0.0035
r_s = 0.95, p = 0.0011
r_p = 0.86, p = 0.0059
r_s = 0.90, p = 0.0046
r_p = 0.95, p = 0.0003
r_s = 0.98, p = 0.0004
Mean protein expression (No. of molecules)
D
increased translation
K_on = 0.01
r_p = 0.98, p= 1.2×10^-5
r_s = 0.93, p= 0.002
K_on = 0.05
r_p = 0.98, p= 1.4×10^-5
r_s = 0.93, p= 0.002
K_on = 0.1
r_p = 0.98, p= 3.2×10^-5
r_s = 0.91, p= 0.005
K_on = 0.5
r_p = 0.97, p= 7.4×10^-5
r_s = 0.88, p= 0.007
K_on = 1.0
r_p = 0.86, p= 0.006
r_s = 0.79, p= 0.028
K_on = 2.0
r_p = -0.18, p= 0.68
r_s = -0.48, p= 0.24
K_on = 5.0
r_p = -0.64, p= 0.09
r_s = -0.50, p= 0.20
K_on = 10.0
r_p = -0.70, p= 0.20
r_s = -0.50, p= 0.20
bursty
uniform
Increased transcriptional burst freq.
Protein noise (CV)
Mean protein expression (No. of molecules)

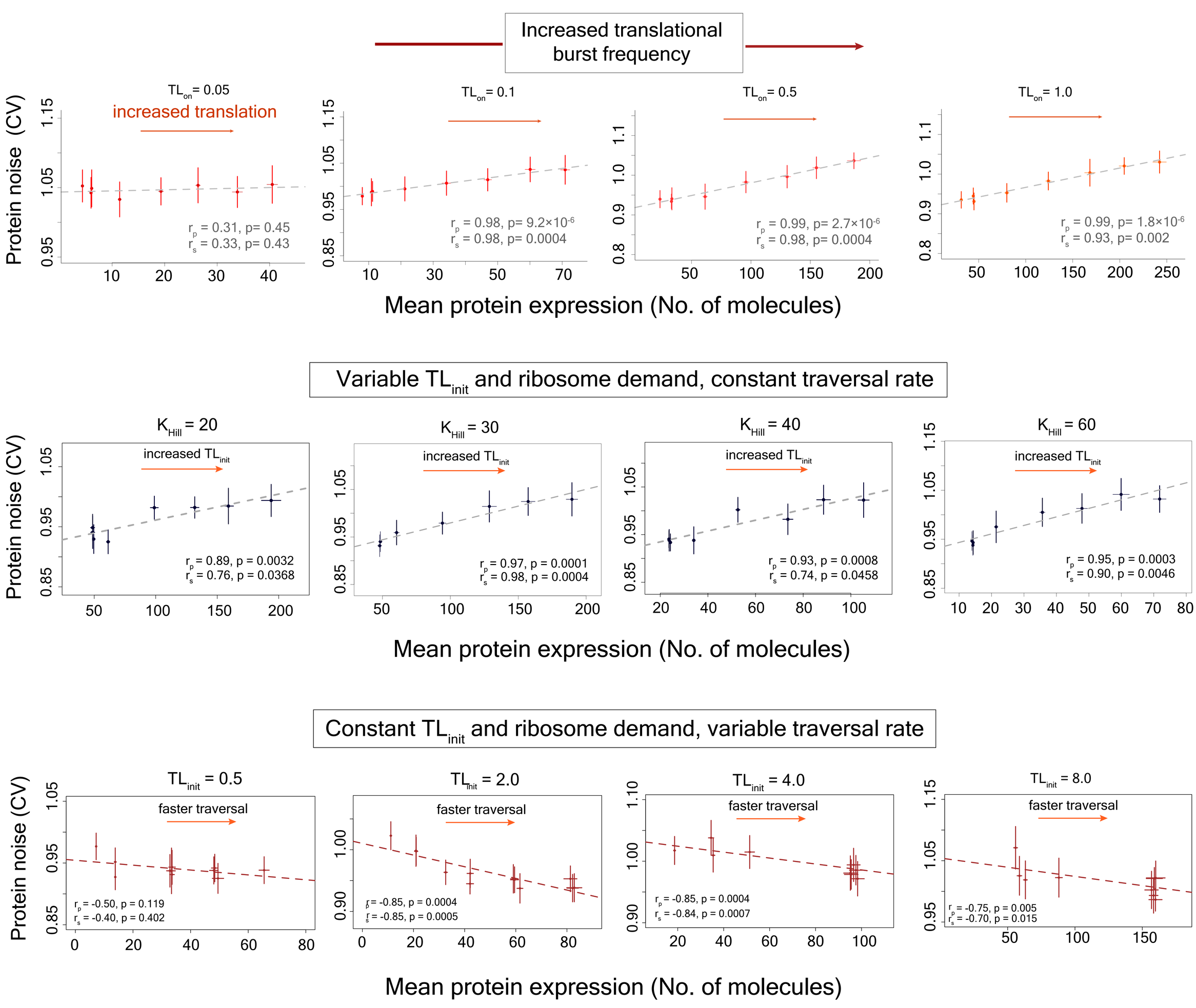
A
Increased translational burst frequency
TL_on = 0.05
increased translation
r_p = 0.31, p= 0.45
r_s = 0.33, p= 0.43
TL_on = 0.1
r_p = 0.98, p= 9.2×10^-6
r_s = 0.98, p= 0.0004
TL_on = 0.5
r_p = 0.99, p= 2.7×10^-6
r_s = 0.98, p= 0.0004
TL_on = 1.0
r_p = 0.99, p= 1.8×10^-6
r_s = 0.93, p= 0.002
Protein noise (CV)
Mean protein expression (No. of molecules)
B
Variable TL_init and ribosome demand, constant traversal rate
K_Hill = 20
increased TL_init
r_p = 0.89, p = 0.0032
r_s = 0.76, p = 0.0368
K_Hill = 30
r_p = 0.97, p = 0.0001
r_s = 0.98, p = 0.0004
K_Hill = 40
r_p = 0.93, p = 0.0008
r_s = 0.74, p = 0.0458
K_Hill = 60
r_p = 0.95, p = 0.0003
r_s = 0.90, p = 0.0046
Protein noise (CV)
Mean protein expression (No. of molecules)
C
Constant TL_init and ribosome demand, variable traversal rate
TL_init = 0.5
faster traversal
r_p = -0.50, p = 0.119
r_s = -0.40, p = 0.402
TL_init = 2.0
r_p = -0.85, p = 0.0004
r_s = -0.85, p = 0.0005
TL_init = 4.0
r_p = -0.85, p = 0.0004
r_s = -0.84, p = 0.0007
TL_init = 8.0
r_p = -0.75, p = 0.005
r_s = -0.70, p = 0.015
Protein noise (CV)
Mean protein expression (No. of molecules)

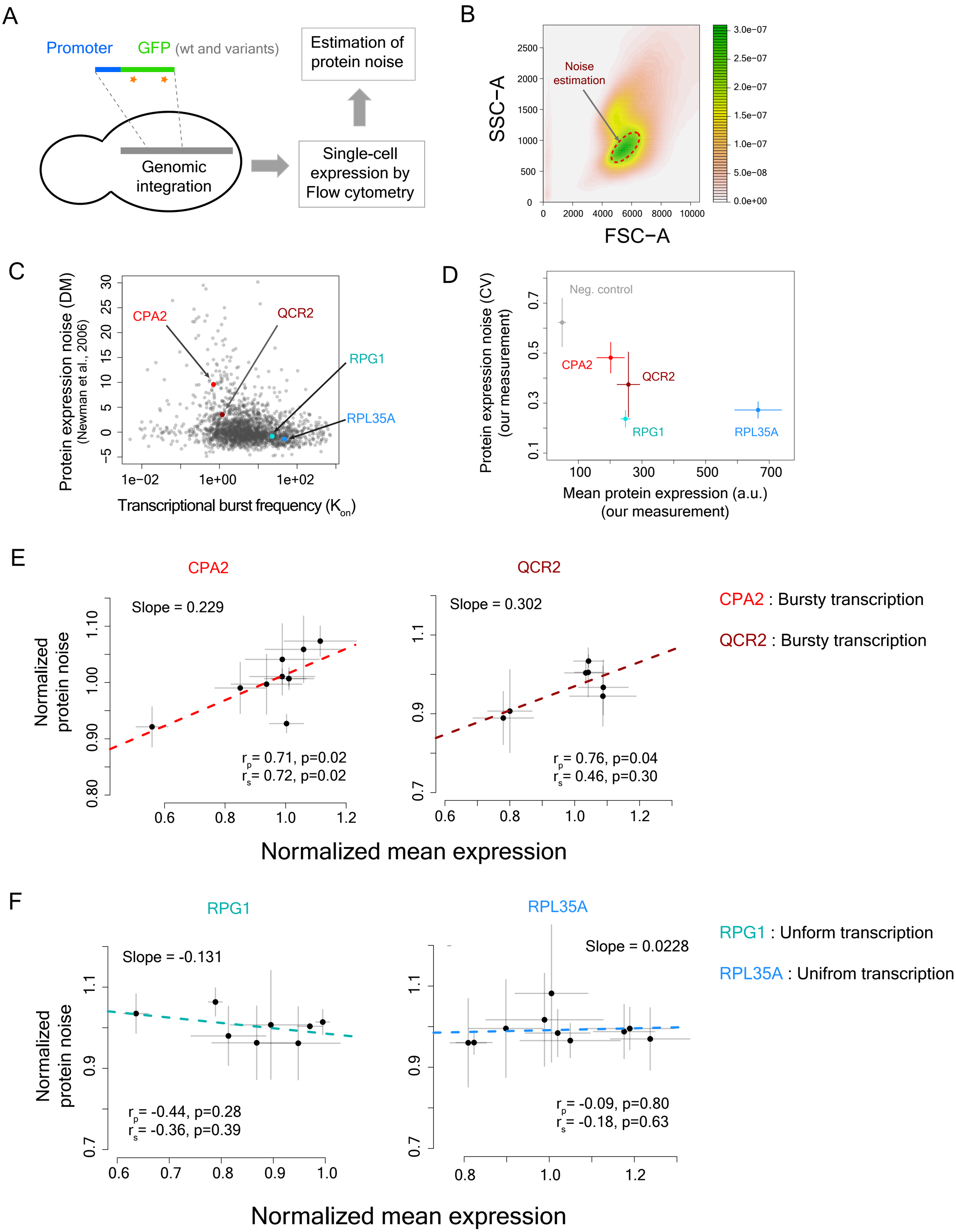
A
Promoter
GFP (wt and variants)
Genomic integration
Single-cell expression by Flow cytometry
Estimation of protein noise
B
Noise estimation
SSC−A
FSC−A
C
CPA2
QCR2
RPG1
RPL35A
Protein expression noise (DM) (Newman et al., 2006)
Transcriptional burst frequency (K_on)
D
Neg. control
CPA2
QCR2
RPG1
RPL35A
Protein expression noise (CV) (our measurement)
Mean protein expression (a.u.) (our measurement)
E
CPA2
Slope = 0.229
r_p = 0.71, p=0.02
r_s = 0.72, p=0.02
QCR2
Slope = 0.302
r_p = 0.76, p=0.04
r_s = 0.46, p=0.30
Normalized protein noise
Normalized mean expression
CPA2 : Bursty transcription
QCR2 : Bursty transcription
F
RPG1
Slope = -0.131
r_p = -0.44, p=0.28
r_s = -0.36, p=0.39
RPL35A
Slope = 0.0228
r_p = -0.09, p=0.80
r_s = -0.18, p=0.63
Normalized protein noise
Normalized mean expression
RPG1 : Unform transcription
RPL35A : Unifrom transcription